UCRL-8311

Chemistry Distribution

UNIVERSITY OF CALIFORNIA

Radiation Laboratory
Berkeley, California

Contract No. W-7405-eng-48

CHEMISTRY OF +1 IODINE IN ALKALINE SOLUTION

Yuan-tsan Chia

(Thesis)

June 2, 1958

Printed for the U. S. Atomic Energy Commission

DISCLAIMER

CHEMISTRY OF +1 IODINE IN ALKALINE SOLUTION

Contents

Contents

(continued)

CHEMISTRY OF +1 IODINE IN ALKALINE SOLUTION

Yuan-tsan Chia

Radiation Laboratory and
Department of Chemistry and Chemical Engineering
University of California, Berkeley, California

June 2, 1958

ABSTRACT

The iodine species formed either by adding hypochlorite to a basic iodide solution or by adding triiodide to sodium hydroxide, was identified as hypoiodite ion. The absorption spectrum of IO^- was investigated in the wavelength range from 450 mμ to 280 mμ.

The kinetics of the reaction

$$I^- + ClO^- = IO^- + Cl^-$$

was studied spectrophotometrically in alkaline solution. The forward rate law was found to be

$$\frac{d(IO^-)}{dt} = \frac{k(I^-)(ClO^-)}{(OH^-)} .$$

At 25°C and an ionic strength of 1.00 M, k is 61 ± 3 sec^{-1}.

It was found spectrophotometrically that for certain ratios of the initial iodide to hydroxide concentrations, there was evidence of the presence of I_3^-, I_2OH^-, and $I_2O^=$ along with IO^-. The equilibrium constants between IO^- and these three species were evaluated by a graphical method.

The formal potential of the cell:

$$Pt : H_2 : 1\ M\ NaOH : 1\ M\ NaOH, KI, NaIO : Au$$

was found to be 1.297 v at 25°C. The equilibrium constant, $K_2 = (I_3^-)(OH^-)^2/(IO^-)(I^-)^2$, of the reaction

$$IO^- + 2I^- + H_2O \rightleftharpoons I_3^- + 2OH^-$$

calculated from emf measurements agreed well with that from spectrophotometric measurements. The ionization constant of HOI was calculated to be 2.3×10^{-11} at 25°C.

I. INTRODUCTION

At first glance it might appear that an element known so long and so intensively studied as iodine would require no further discussion; however, the aqueous solution chemistry of this element in the +1 oxidation state has not been well defined. For example, no reliable values of the ionization constant of HOI and the potential of the I^- - IO^- couple in basic solution have been reported in the literature. In acid solution the species H_2IO^+ has been suggested as one of the products of the hydrolysis of iodine,[1,2] yet little evidence has so far been obtained for its existence. Because in aqueous solution the oxygen atom in the water molecule appears to be more negative than that in hypoiodous acid, as judged from the ionization constants, it seems questionable whether H_2IO^+ does in fact exist in preference to H_3O^+. Therefore it is evident that further research will be necessary before the +1 iodine chemistry can be considered well established.

Initially it was hoped that the species IO^- and HOI of +1 iodine could be prepared in alkaline solution and studied spectrophotometrically to give the spectra and ionization constant of HOI. The spectrum of this latter species could be used as a starting point for the spectrophotometric investigation of H_2IO^+.

The work reported here was carried on in alkaline solution and consists of (a) the preparation and identification of IO^-; (b) a kinetic study of the formation of IO^- from I^- and ClO^-; (c) spectrophotometric studies of the equilibria between IO^-, I_3^-, I^-, I_2OH^-, and $I_2O^{=}$; (d) emf measurement of the I^- - IO^- couple and (e) determination of the ionization constant of HOI.

II. APPARATUS AND EQUIPMENT

All absorbances (optical densities) were measured on either a model 11, serial 4 Cary recording spectrophotometer or a Beckman model DU spectrophotometer. The wavelength scale of the former was checked against the emission spectra from hydrogen and mercury-discharge tubes as well as the Fraunhofer lines in the spectrum of the sun. The wavelength scale of the latter was checked against a mercury-discharge tube. The solution samples were contained in quartz absorption cells while the absorbances were being measured. The absorbance of a material was obtained by running the spectrum versus air and then, using the same cell, measuring the absorption due to the blank solution (in most cases water) also versus air. Subtraction of the two absorption curves gave the absorption due to the material in the solution. The scale of absorbance on the Beckman Spectrophotometer could be read to 0.002, that of the Cary to 0.005.

The emf measurements and the mixing process of all experiments were carried out in a 25°C thermostated water bath, constant to $\pm$ 0.01°C.

The cell used in the emf measurements is shown in Fig. 1. It was made of Pyrex glass with ground-glass joints. It was designed to measure the potential of the I^- - IO^- couple in the internal cell compartment (A) with hydrogen electrodes (B_1, B_2) as reference electrodes. The hydroxide concentration in (A) was made the same as that in the external cell compartment (C). Cell (A) was a glass container of about 50 ml volume to level (D). The bottom part of (E) of (A) was removable by means of a ground-glass joint. The contact of the two half cells was made through the thin film of liquid in the joint. Cell (A) had a top with three openings (G_1, G_2, G_3). Two of the openings were for the

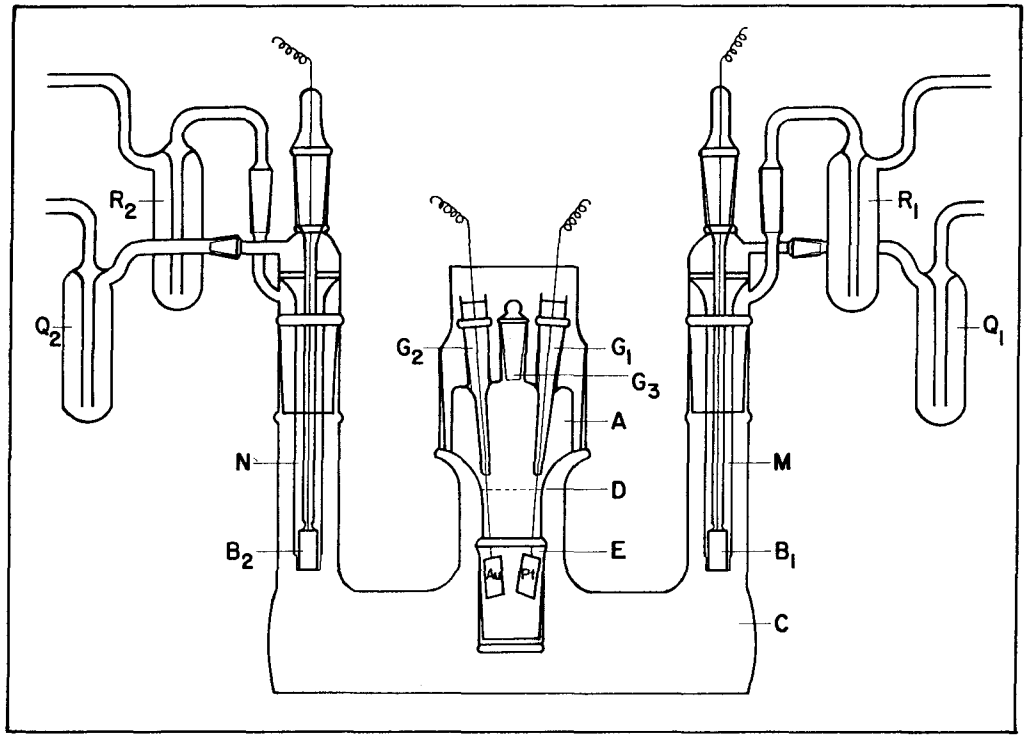

Fig. 1. The cell used in the emf measurements.

platinum and gold electrodes. The third one was for a funnel for transferring solution, and was stoppered when not in use. The gold and platinum electrodes were foils about 1 by 2 cm in area. They were cleaned by dripping with freshly condensed CCl_4 vapor on the electrodes. The leads from the two electrodes to the contact tubes were made long enough so that the two electrodes and wires would be immersed below level (D) when a 50-ml sample was put into (A). The leads from all electrodes (including the two hydrogen electrodes) were sealed in solid glass and were connected directly to the wire leads to the potentiometer, with no mercury being used for making the contacts. In the case of the gold electrode, a gold wire about 4 cm in length was used to connect the electrode to a platinum wire, which was sealed into glass. The electrodes were stored in conductivity water when not in use. The volume of the solution put into cell (C) was about 500 ml. The hydrogen inlet (Q_1, Q_2) and outlet (R_1, R_2) bubblers were about 30 ml in volume. About 20 ml of the same solution as in (C) was put into both Q_1 and Q_2, while about 10 ml was introduced into R_1 and R_2. The level of the solution in Q_1 was adjusted to equal that of Q_2 and that of R_1 to equal R_2.

The two hydrogen electrodes were platinum foils of about 1 by 2 cm in area. They were not prepared in an absolutely identical manner on purpose.[3] The old platinum black was removed by dipping the electrodes into aqua regia for a few minutes. The electrodes were platinized in a 2% platinic chloride solution containing 0.02% of lead acetate.[3] A current density of 60 milliamp/cm^2 was applied with gentle stirring and a reversal of polarity every half minute. The total time used on platinization was from 5 to 7 minutes. The electrodes were then electrolyzed in a 0.2 $\underline{M}$ H_2SO_4 solution for half an hour with the same

procedure as used in platinization. Finally the electrodes were soaked in conductivity water for about an hour before they were put into the cell.

The potential of the cell was measured with a Rubicon type-B, high-precision potentiometer with a dc spotlight galvanometer (sensitivity 0.01 ua/mm, period 4.0 sec, and critical-damping resistance 190 ohms) for indication of the null point. The potentiometer was checked against a Weston standard cell from time to time during an experiment.

A stopwatch that could be read to 1/5 sec was used for all the experiments to record time. The time record was supplemented by the use of the running speed of the spectrophotometer's chart paper, which was found to be 5.00 ± 0.02 sec per division.

The apparatus used in the "injection method" will be reported under that subject.

III. PREPARATION AND ANALYSIS OF REAGENTS

Conductivity water, prepared by redistilling distilled water from alkaline permanganate solution in a Barnstead still, was used for making all solutions. All solid chemicals were reagent grade.

The hypochlorite solution was prepared by passing tank chlorine into a standardized sodium hydroxide solution, until the pH of the solution was about 12 (measured with a Beckman model-G pH meter). The concentration of the hypochlorite solution was determined iodometrically by forming triiodide from hypochlorite and iodide in a dilute sulfuric acid solution and titrating the triiodide with standard sodium thiosulfate using starch as the indicator. The concentration of iodide ion and hydrogen ion were both adjusted to 0.1 M for the titration. The sodium thiosulfate solution was standardized against potassium iodate. The concentration of hypochlorite solution was usually checked before each experiment. At most, a very slow decrease in concentration was found.

The sodium hydroxide solution was prepared by diluting saturated sodium hydroxide with cold, freshly boiled conductivity water. It was standardized against a standard hydrochloric acid solution.

The iodide solution used in all experiments was freshly prepared by dissolving a weighed amount of potassium iodide in the desired amount of water. Potassium iodide was used in most of the experiments. When $NaClO_4$ was used to keep the ionic strength constant, sodium iodide was used.

The sodium perchlorate solution was prepared by treating analytical-grade sodium carbonate with a small excess of double-vacuum-distilled perchloric acid. The solution was boiled to expel carbon dioxide, and the acidity was adjusted to a pH of 5 or 6 with a pH meter by addition of carbonate-free sodium hydroxide. The resulting $NaClO_4$ solution was

standardized by evaporating aliquots to dryness in a platinum crucible and weighing as $NaClO_4$ after drying at 150°C for 2 hr.

The sodium chloride solution used in adjusting the ionic strength was prepared by drying "Mallinckrodt" analytical reagent salt at 110°C, then dissolving a weighed amount of the salt in the desired amount of water.

The triiodide solution was prepared by weighing solid iodine in a concentrated potassium iodide solution, and diluting the triiodide solution with desired amount of water. Aliquot portions of the resulting solution were titrated against standard sodium thiosulfate solution with both concentrations of iodide and hydrogen ion adjusted to 0.1 M. The concentration compared well with that calculated from the initial weighing.

Very pure hydrogen, prepared by electrolysis of water and passed over platinum sponge and hot nickel catalyst, as well as through a cold trap, was used.

The alkaline pyrogallol solution used was made by dissolving 15 g of pyrogallic acid in 100 ml of 50% KOH solution.

IV. +1 IODINE SPECIES IN 1 M OH^- SOLUTION - THE HYPOIODITE ION

(A) Preparation

It has been reported that hypoiodite ion can be prepared by mixing triiodide ion with an alkaline solution.[4,5,6] Comparing the oxidation potential of the Cl^- and ClO^- couple to that of I^- and IO^-, one predicts the formation of IO^- by the reaction of I^- and ClO^-. In this investigation both methods were used to prepare IO^-.

(1) Experimental Procedure

(a) The mixing process. A measured volume of the basic iodide solution (no iodide was present in the case of IO^- prepared by $I_3^- + OH^-$) of known concentration and a standardized solution of hypochlorite (or I_3^-) were placed in separate glass-stoppered flasks and were brought to $25.00 \pm 0.01^\circ C$ by immersion in a thermostated water bath for over an hour. The flasks were covered with aluminum foil to exclude light. Added chloride ion or perchlorate ion was contained in the flask of basic iodide solution for experiments in which the ionic strength was kept constant. The reaction was started by adding the desired volume of ClO^- (or I_3^-) through a calibrated pipet to the basic iodide (or OH^- only) while the latter was being stirred vigorously by an electric stirrer. The pipet used for some of the experiments had a delivery time of less than 5 sec. The zero time was taken at the start of the addition of ClO^- (or I_3^-). Experiments were done with reversal of the order of mixing (i.e. by adding I^- to ClO^-), but no effects were observed.

(b) Spectrophotometric measurements. A pipet with a large opening at the delivery end was used to transfer the reaction mixture from the mixing flask to the absorption cell, which had been placed in the cell compartment before the mixing process. The volume of the pipet was

slightly larger than the volume of the absorption cell used and the wide-open orifice just fitted the opening of the cell. The time required from the zero time to the first spectrophotometric measurement was usually about 1 min.

To make the spectrophotometric measurements, the air blank was checked first. The recording of the absorption spectrum of the sample solution usually was started at 400 mμ and went down in wavelength to where the absorbance exceeded 3.4, usually between 240 mμ and 280 mμ. The scanning was repeated at appropriate time intervals. For experiments in which the disproportionation of hypoiodite ion was rapid, the spectrophotometric scannings were carried on one right after another.

(2) The Absorbance-time Curves for a Typical Experiment

The values of the absorbance of the sample solution (i.e. the difference between the observed absorbance and the absorbance of conductivity water) at one wavelength was plotted against time, the absorbance of the sample solution at zero time at that wavelength was obtained by extrapolation. The absorbance-time (A-t) curves at 400.6 mμ and 360.5 mμ for a typical experiment are shown in Fig. 2.

(3) The Solid Iodine Method

Attempts were made to prepare IO^- by the hydrolysis of solid iodine in alkaline solution. A wide-mouth reaction flask which contained the desired volume of standard sodium hydroxide solution was thermostated in a 25.00 $\pm$ 0.01°C water bath for over an hour, then a freshly weighed, well-ground sample of solid iodine in a weighing bottle was held barely above the solution level of the reaction flask. The weighing bottle had a wide mouth and was very short. The reaction was started by opening the stopper of the weighing bottle and quickly pouring the solid iodine

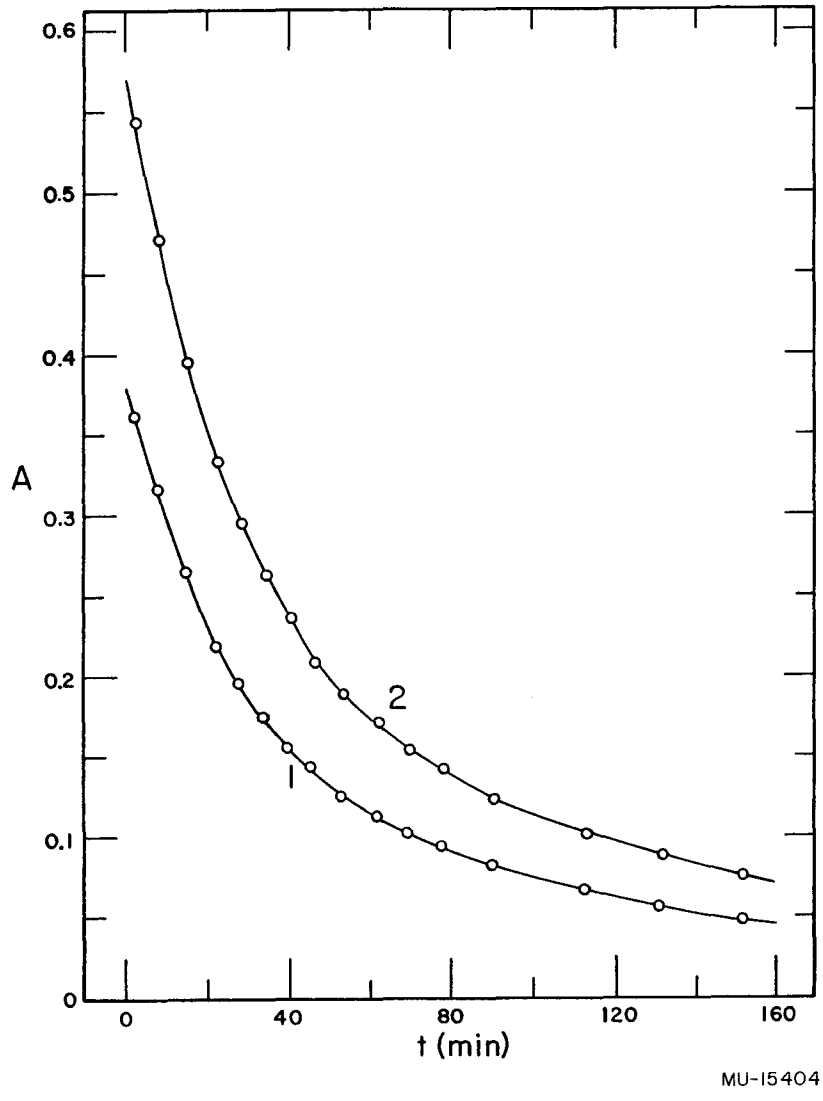

Fig. 2. The absorbance-time curve for a typical experiment (Experiment I-J-6). Curve 1 : λ = 400.6 mμ ; Curve 2 : λ = 360.5 mμ.

into the reaction flask while the latter was being stirred. The stirrer was temporarily stopped for a second or so to drop the empty weighing bottle and stopper into the reaction flask. The zero time was recorded as the time of adding the solid iodine. By experience, the time required for the disappearance of 1 g of solid iodine in 500 ml of 1.00 M OH^- was about 40 sec; therefore this was the time allowed in experiment III-M-1 before a sample was taken out for spectrophotometric measurement. The initial concentration of iodine of that experiment was 0.01007 M and that of OH^- was 1.020 M. The extrapolated value of the absorbance at zero time at 400.6 mμ from the A-t curve was found to be 0.200.

(B) Identification

In order to make sure that the iodine species prepared by the two methods mentioned above (i.e. I_3^- + OH^- and I^- + ClO^- + OH^-) was in the +1 oxidation state, a series of experiments was run keeping the initial hydroxide concentration at 1.000 M and varying the concentrations of I^- as well as ClO^-. The results are listed in Table I. The headings are self-explanatory except for $\bar{\epsilon}$, which is defined as the effective molar absorptivity (Extinction coefficient), or $\bar{\epsilon} = A_o/b\Sigma$, where A_o represents the absorbance at zero time, Σ is the initial concentration of ClO^- (or I_3^-) in moles per liter, and b is the length in centimeters of the cell used in that experiment. The uncertainty of the value of $\bar{\epsilon}$ depends on the initial slope of the A-t curve and how soon the first point was measured. The rates of disproportionation of IO^- of all experiments of Table I were not too fast to permit a fairly good extrapolation. The $\bar{\epsilon}$ values at 400.6 mμ, 360.5 mμ and 320.1 mμ are believed to be accurate within 3%, and that for 289.9 mμ may be somewhat more uncertain. The values of $\bar{\epsilon}$ in Table I at the four wavelengths were plotted against

Table I

The effective molar absorptivities at zero time of solutions of iodide oxidized by hypochlorite*

No. of Exp't.	$(ClO^-)_{in}$ ($\times 10^3$ M)	$(I^-)_{in}$ ($\times 10^3$ M)	$\frac{(I^-)_{in}}{(ClO^-)_{in}}$	Cell Length (cm)	$\bar{\epsilon}_{400.6}$	$\bar{\epsilon}_{360.5}$	$\bar{\epsilon}_{320.1}$	$\bar{\epsilon}_{289.9}$
II-C-2	6.000	2.000	0.3333	5	12.1	24.5	130.0	276
II-C-1	4.000	2.000	0.5000	5	17.9	31.5	116.6	260
I-J-6	10.00	10.00	1.000	1	38.5	57.1	47.6	134.3
III-P-1	9.017	10.00	1.109	1	38.8	58.8	49.2	141.0
III-A-3	1.803	2.500	1.387	5	37.7	57.4	47.4	129.5
III-A-4	1.803	4.000	2.218	5	37.6	58.0	48.0	-
III-G-5	+1.803	3.141	**4.742	5	38.3	56.0	46.8	132.2
III-H-I	1.803	8.950	4.964	5	40.5	61.0	48.7	140.0
III-G-3	+1.810	3.676	**5.030	5	38.2	56.8	46.9	136.3
III-G-4	+1.800	3.655	**5.030	5	38.0	59.0	51.9	143.8

*$(OH^-)_{in}$ = 1.000 M

+The reported value is initial triiodide concentration.

**The reported value represents $[(I^-)_{in} + 3(I_3^-)_{in}]/(I_3^-)_{in}$.

$(I^-)_{in}/(ClO^-)_{in}$ (or $[\ (I^-)_{in} + 3(I_3^-)\ ] / (I_3^-)_{in}$) as shown in Figs. (3) and (4). The subscript "in" indicates initial concentration in moles per liter. All four plots show that the effective molar absorptivity varies linearly with respect to $(I^-)_{in}/(ClO^-)_{in}$ from zero to the point where the ratio of (ClO^-) to (I^-) was 1; then when the ratio changed from 1 to 5, the values of $\bar{\epsilon}$ remained constant within experimental error. The break at the point where $(I^-)_{in}/(ClO^-)_{in} = 1$ gives evidence that the main species formed in both methods of preparation was in the +1 oxidation state. It will be shown later that this species is IO^-.

(C) Absorption Spectra of IO^-, ClO^-, I_3^-, IO_3^-, and I^-

(1) The Absorption Spectrum of IO^-

The molar absorptivity of IO^- at wavelengths other than 400.6 mμ was calculated by using the A-t curve at 400.6 mμ and the following equation:

$$A_o^{\lambda} = A_t^{\lambda} A_o^{400.6} / A_t^{400.6} \quad . \tag{1}$$

The superscript indicates the wavelength in millimicrons and the subscript the time after mixing. The spectrophotometric results of Experiment I-J-6 were used for the calculation and are listed in Table II. The values of the molar absorptivity of IO^- at 360.5 mμ, 320.1 mμ and 289.9 mμ calculated from Eq. (1) agree with the corresponding extrapolated values from the A-t curves at those wavelengths within experimental error. This gives justification for the use of Eq. (1) to calculate the values of A_o for those wavelengths at which no A-t curves have been plotted. The absorption spectrum of IO^- from 450 mμ to 280 mμ is shown in Fig. (5).

(2) The Absorption Spectrum of ClO^-

The absorption spectrum of ClO^- was studied by measuring the absorbances of standard ClO^- solutions with the Cary recording spectrophotometer

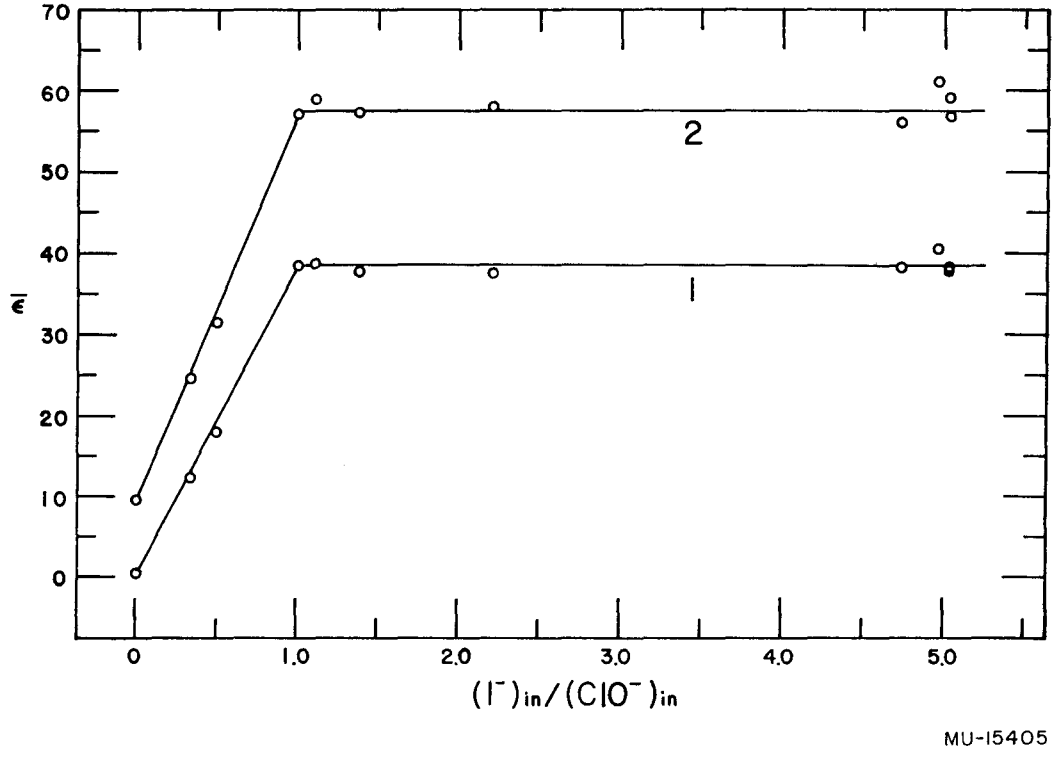

Fig. 3. Plot of $\bar{\epsilon}$ vs $(I^-)_{in}/(ClO)_{in}$.
Curve 1 : λ = 400.6 mμ ; Curve 2 : λ = 360.5 mμ.

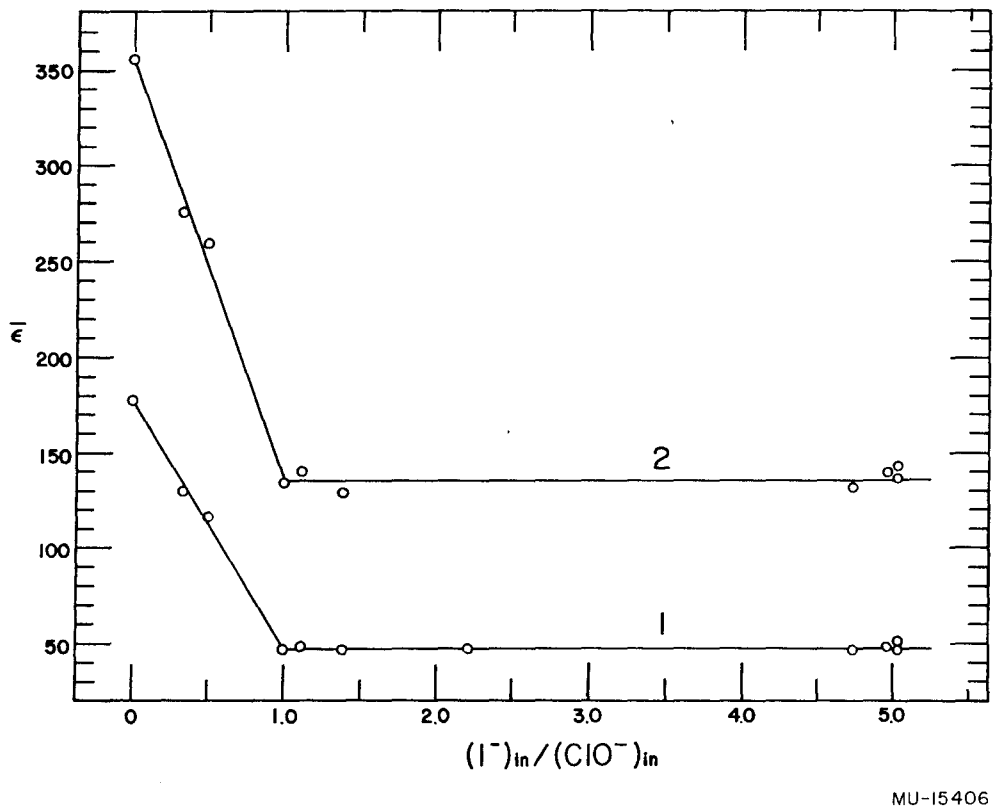

Fig. 4. Plot of $\bar{\epsilon}$ vs $(I^-)_{in}/(ClO^-)_{in}$.
Curve 1 : λ = 320.1 mμ ; Curve 2 : λ = 289.9 mμ.

Table II

The molar absorptivities of hypoiodite and hypochlorite ions

λ (mμ)	ϵ_{IO^-}	ϵ_{ClO^-}
450.3	9.45	-
425.4	20.0	-
400.6	38.5	0.510
393.0	45.7	0.730
382.2	54.7	1.580
371.6	59.6	3.86
360.5	57.1	9.80
350.8	53.9	22.8
340.5	49.6	52.9
330.2	47.7	102.8
320.1	47.6	178.0
310.0	54.3	266
299.9	79.6	337
289.9	134.3	356
280.0	224	304
270.0	-	201
260.0	-	104.5
250.0	-	44.0
240.0	-	17.41

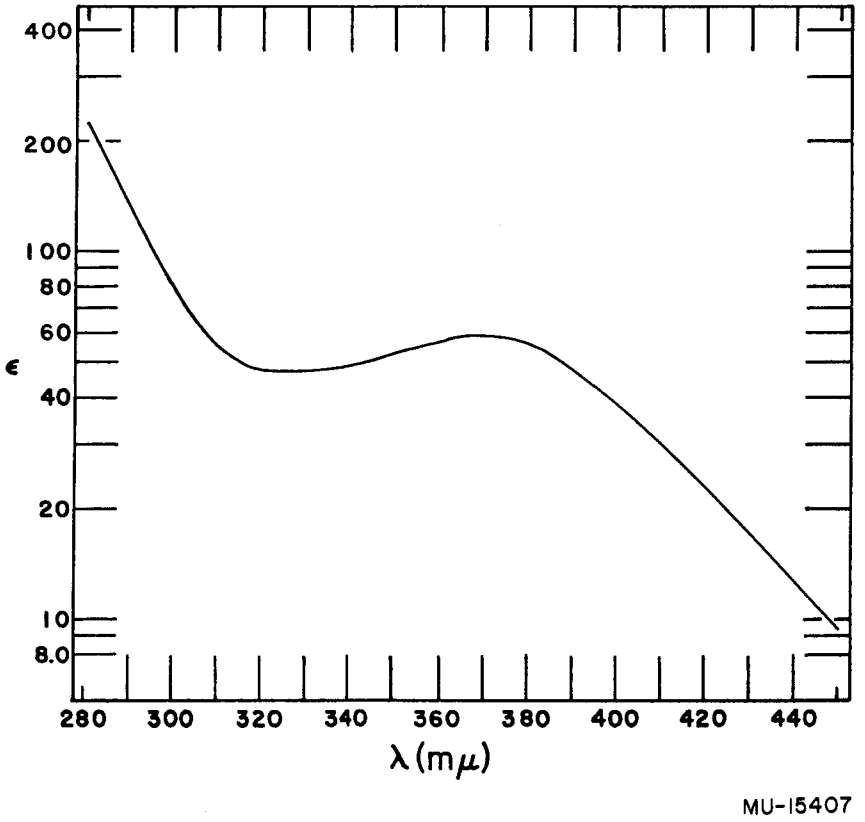

Fig. 5. The absorption spectrum of hypoiodite ion.

in the wavelength range from 400 mμ to 240 mμ. The values of the molar absorptivities are listed in Table II and the absorption spectrum is shown in Fig. 6.

The absorption spectrum of ClO^- was previously studied by Friedman;[7] however, in order to obtain more precise values of the molar absorptivities, it was considered desirable to investigate it again. Over the wavelength region from 340 mμ to 270 mμ, the shape of the absorption curve from Friedman's results agreed with that from this investigation, but the molar absorptivities from the plot given by Friedman were about 10% lower than those obtained in this work. Then from 260 mμ to 240 mμ Friedman's results of the molar absorptivities became higher than the values reported here. The discrepancy at 240 mμ was about 50%.

(3) The Absorption Spectra of IO_3^- and I^-

Awtrey and Connick studied the absorption spectra of IO_3^- and I^- in the wavelength range from 215 mμ to 270 mμ (or 260 mμ in the case of I^-).[8] Because both I^- and IO_3^- are the final products of the disproportionation of IO^-, it was thought worthwhile to study the absorption spectra of these two ions in the wavelength range from 280 mμ to 400 mμ, which is the region where this investigation has been conducted. These spectra were investigated by measuring the absorbances of the solutions of potassium salts of known concentrations with the Beckman model DU spectrophotometer. The solutions had been centrifuged before they were introduced into the absorption cells. In the case of iodide, several solutions were prepared from KI salts of different manufacturers; these were potassium iodide solutions with or without trace amounts of $S_2O_3^=$, KI in 1.000 M OH^-, and KI in 1.000 M KCl. Due to the very small absorptions of iodide in this wavelength range, and the possible contamination by trace amounts

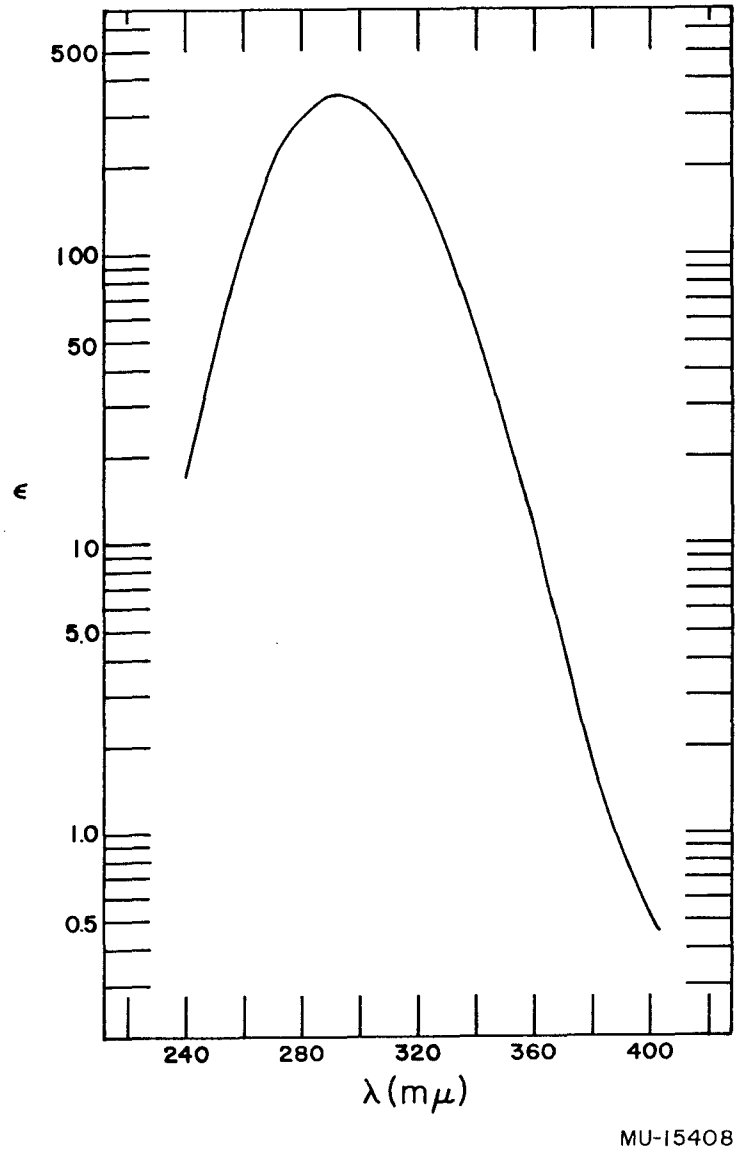

Fig. 6. The absorption spectrum of hypochlorite ion.

of I_3^- in some of the above cases, attempts to get accurate values of ϵ_{I^-} at the higher wavelengths were not successful. Therefore only upper limits of ϵ_{I^-} are given in Table III from 290 mμ to 320 mμ. From 330 mμ to 400 mμ, the value of ϵ_{I^-} was found to be less than 0.006. Because of the same difficulties of small absorbances, only upper limits of the absorptivities of IO_3^- are listed in Table III from 290 mμ to 340 mμ.

(4) The Molar Absorptivity of I_3^- and Its Linear Variation with (I^-)

The absorption spectrum of I_3^- was studied by Awtrey and Connick[8] in I_3^- solutions containing 0.049 M I^- from 270 mμ to 590 mμ. For studies to be discussed later, it was necessary to measure the absorption spectrum of triiodide ion as a function of iodide concentration.

(a) Experimental procedure. Five aliquots of standard triiodide solution were diluted with conductivity water containing different weighed amounts of potassium iodide. The concentration of I^- in the final solutions ranged from 0.1 M to 1 M. The dilute triiodide solution was transferred to a gas-washing bottle and was maintained at 25.00 ± 0.01°C in a water bath for about 1 hr. During this period, carbon dioxide gas was passed slowly into the air space over the solution in the washing bottle to avoid air oxidation. Finally the washing bottle was shaken, and a sample of the triiodide solution was introduced into a 1-cm ground-glass-stoppered quartz cell for spectrophotometric measurement. The cell was filled as completely as possible to avoid air. The absorption spectra from 400 mμ to 280 mμ of these triiodide solutions were measured by the use of the Cary recording spectrophotometer. The values of absorbances at 400.6 mμ and 360.5 mμ were checked with the Beckman model DU spectrophotometer. A constant-temperature cell holder

Table III

The molar absorptivities of iodide and iodate ions

λ (mμ)	$\epsilon_{I^-} \times 10^3$	$\epsilon_{IO_3^-} \times 10^2$
340.4	-	< 3
330.3	-	< 3
320.3	< 8	< 4
310.3	< 10	< 7
300.2	< 15	< 20
290.2	< 29	< 100
280.1	161	520

was used with the latter to keep the temperature of the cell compartment at 25°C. No deviation was ever found in the results of molar absorptivities at 360.5 mμ and 400.6 mμ from the two different machines.

(b) Results. From the above experiments it was noticed that at different iodide concentrations the absorption peaks of I_3^- remained at the same wavelengths, but the molar absorptivities (after correction for the absorption due to I^-) varied with the iodide concentration. The values of $\epsilon_{I_3^-}$ at 400.6 mμ, 360.5 mμ, 320.1 mμ, and 289.9 mμ were plotted against I^- concentration. A straight line was obtained within the experimental accuracy at each of the four wavelengths. The plot at 360.5 mμ is shown in Fig. 7. As a consequence, the molar absorptivity of I_3^- can be expressed as

$$\epsilon_{I_3^-} = \epsilon_{I_{3_0}^-} + \alpha(I^-),$$

where $\epsilon_{I_{3_0}^-}$ is the molar absorptivity of I_3^- at zero iodide concentration and α is a constant. The values of $\epsilon_{I_{3_0}^-}$ and α at the four wavelengths mentioned above are reported in Table IV.

Table IV

Parameters for the equation: $\epsilon_{I_3^-} = \epsilon_{I_3^-_0} + \alpha(I^-)$

λ (mμ)	$\epsilon_{I_3^-_0} \times 10^{-3}$	$\alpha \times 10^{-3}$
400.6	5.99	1.93
360.5	24.6	4.1
320.1	14.0	2.1
289.9	40.0	-3.8

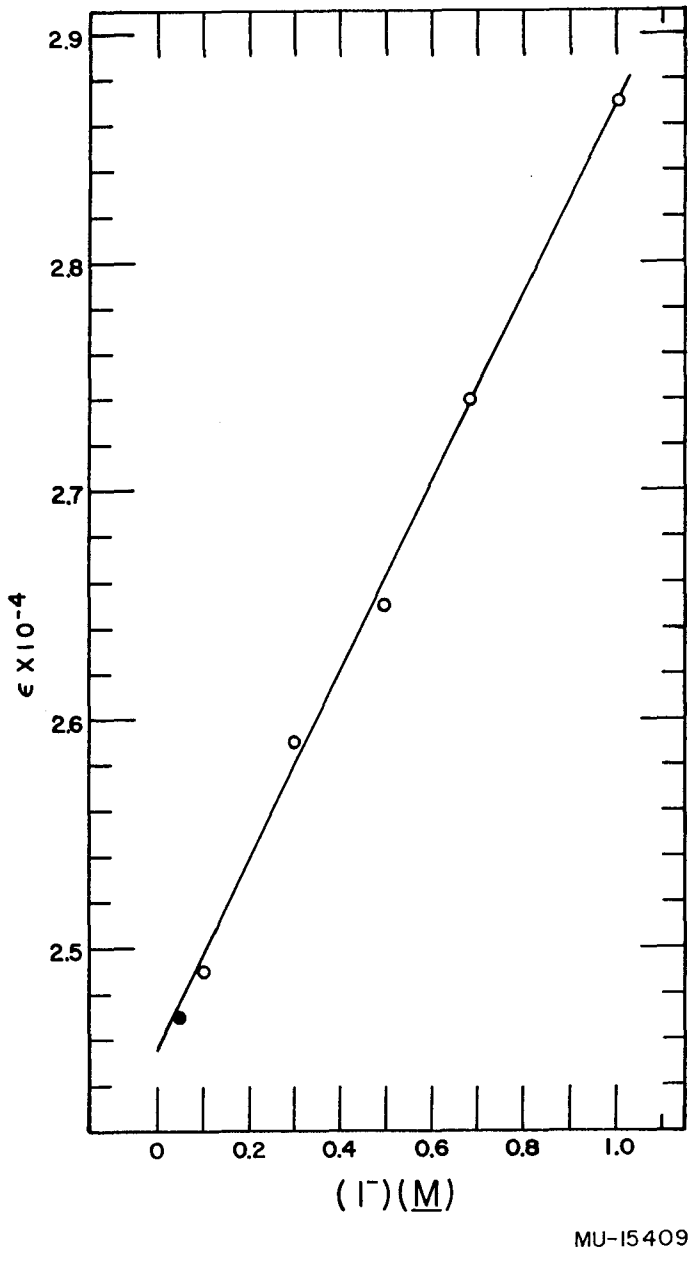

Fig. 7. Plot of ϵ of I_3^- vs iodide concentration. λ = 360.5 mμ.

(D) Discussion

As indicated in Table I as well as in Figs. 3 and 4, the effective molar absorptivities obtained from preparing IO^- by the hydrolysis of I_3^- in alkaline solution agreed very well with those obtained from mixing ClO^- in base with iodide. However, when solid iodine was dissolved into 1.000 M OH^- as a third method of preparation, the absorbance at zero time at 400.6 mμ from the extrapolation of the A-t curve was only a little bit over half of the values from the two other methods. This observation was reproducible and was also true at other wavelengths. Nevertheless the shape of the absorption spectrum from the solid iodine method was the same as those from the other two methods. It is inferred that the absorbing species produced by the solid iodine method was also IO^-, but the concentration of it at the so-called "zero time" was smaller than in the other two cases. A possible explanation for this difference was thought to be related to the dissolution process. During the process of dissolving solid iodine in alkaline solution there would be a considerable decrease in basicity at the surface of the iodine because hydroxide ion is consumed. As the hydroxide concentration decreases, the rate of disproportionation of IO^- increases, so that it is likely that appreciable disproportionation occurred during the dissolution.

The absorption spectrum of IO^- in the wavelength range below 280 mμ has not been carefully studied in the present investigation, because difficulty was experienced in using a 1-mm absorption cell to study spectrophotometrically an IO^- solution that had the same initial concentrations of OH^-, ClO^-, and I^- as those in Experiment I-J-6 of Table I. The rate of the disproportionation of IO^- shown from the A-t

curve when a 1-mm cell is used was found to be about ten times faster than that shown with a 1-cm cell, while all the other conditions were the same. Experimentally it was found that the effect of surface catalysis on the disproportionation of IO^- and the surface effect on the mixing process were both negligible by comparing the behavior of stirred and unstirred solutions. It was observed, however, that light speeds up the disproportionation. The effect of ultraviolet light on the rate of the disproportionation was inversely proportional to the amount of material present. The thicker the cell, the more hypoiodite present and the smaller the light effect. For this reason, the flask of ClO^- (or I_3^-) and the flask where the mixing process took place were always covered with aluminum foil.

The absorption spectrum of I_3^- was found to be a linear function of the I^- concentration in the wavelength range from 400 mμ to 280 mμ. Whether this was due to the presence of another species or was simply a "solvent" effect caused by changing iodide concentrations cannot be stated at the moment. The solid circle in Fig. 7 was the value from Awtrey and Connick[8] and was found to be in good agreement with the extrapolated value from this work.

V. THE RATE OF FORMATION OF IO^- FROM I^- AND ClO^- IN ALKALINE SOLUTION

(A) Introduction

During the investigation of the absorption spectrum of hypoiodite ion at initial iodide and hypochlorite concentrations of both 2.00×10^{-3} M or lower and 1.000 M OH^-, an unusual phenomenon was observed. As shown in Fig. 2, ordinarily the absorbance that was due to IO^- decreased with time; however in this unusual case, a maximum absorbance at 400.6 mμ and 360.5 mμ was found about 6 min after the ClO^- was added. This phenomenon was not observed at 320.1 mμ. The absorption curves from 400 mμ to 280 mμ at times after the time of appearance of the maximum matched well with the absorption spectrum of IO^- obtained previously. The appearance of the maximum absorbance was reproducible and was present when the initial hydroxide concentration was changed to 0.500 M. It was also found that sodium hydroxide from different manufacturers gave the same phenomenon. Table V summarizes the experimental results at 400.6 mμ and 360.5 mμ of those experiments that gave absorbances with maxima. In order to minimize the effect of any impurities in the reagents at these quite low ClO^- and very high OH^- initial concentrations, a hypoiodite solution was prepared under the same conditions as those in Experiment II-B-1 of Table V, and let stand at room temperature in the darkness for 125 hrs. At the end of this period, a sample of this solution was tested spectrophotometrically to make sure that almost all the hypoiodite ion had been disproportionated. A desired amount of ClO^- solution was added to a measured volume of the aged solution. The spectrophotometric data were obtained as usual and again the maximum was observed (Experiment IV-A-2-c of Table V).

Table V

Lower limits of $\bar{\epsilon}$ for experiments showing maxima in the absorbance vs time plots

Exp't No.	$(ClO^-)_{in}$ (x 10^3 M)	$(I^-)_{in}$ (x 10^3 M)	$(OH^-)_{in}$ (M)	Cell length (cm)	$\bar{\epsilon}^{400.6}$	$\bar{\epsilon}^{360.5}$
II-B-1	2.000	2.000	1.000	5	> 36.4	> 55.0
III-R-1	1.803	2.000	1.000	5	> 38.0	> 57.4
III-A-1	1.803	1.500	1.000	5	> 30.5	> 46.2
II-W-1	2.000	2.000	0.5000	5	> 35.9	> 56.1
IV-A-2-c	2.000	1.856	0.9346	5	> 37.4	> 55.7

The A-t curves at 400.6 mμ and 320.1 mμ of Experiment IV-A-2-c are given in Fig. 8. By comparing the molar absorptivities of IO^- (Table II) at 400.6 mμ and at 320.1 mμ to those of ClO^-, one notices that at 400.6 mμ IO^- absorbs much more strongly than ClO^-, but at 320.1 mμ the molar absorptivity of ClO^- is greater than that of IO^-. Therefore, the simplest explanation of the maxima is that the rate of formation of IO^- from I^- and ClO^- is measurable under the conditions used in all experiments of Table V. Accordingly it seemed desirable to investigate further the rate of this reaction. In order to get fast and adequate mixing, the injection method, which had been used by Stern and DuBois[9] as well as by Below[10] was chosen to study this reaction.

(B) The Injection Method

(1) Apparatus

The absorption cell used for mixing and observation was the same as that used by Below.[10] It was a (2.15 ± 0.01)-cm cylindrical cell made of Pyrex with quartz windows. It had a neck about 2 cm in diameter and 2.5 cm high to avoid splashing of liquid. The cell capacity (to the lower end of the neck) was about 9 ml. The length of the cell was checked by calibrating it against another 2-cm cell using a dilute potassium chromate solution.

As was found by Below, too large a needle bore gave poor results because the flow velocity is too small for adequate mixing.[10] On the other hand, too small a needle made it impossible to deliver the 2 ml of solution in less than 1 sec without rupturing the syringe. As in Below's work, a #16 hypodermic needle was used for all the experiments in this investigation without any attempt to use other kinds of needles.

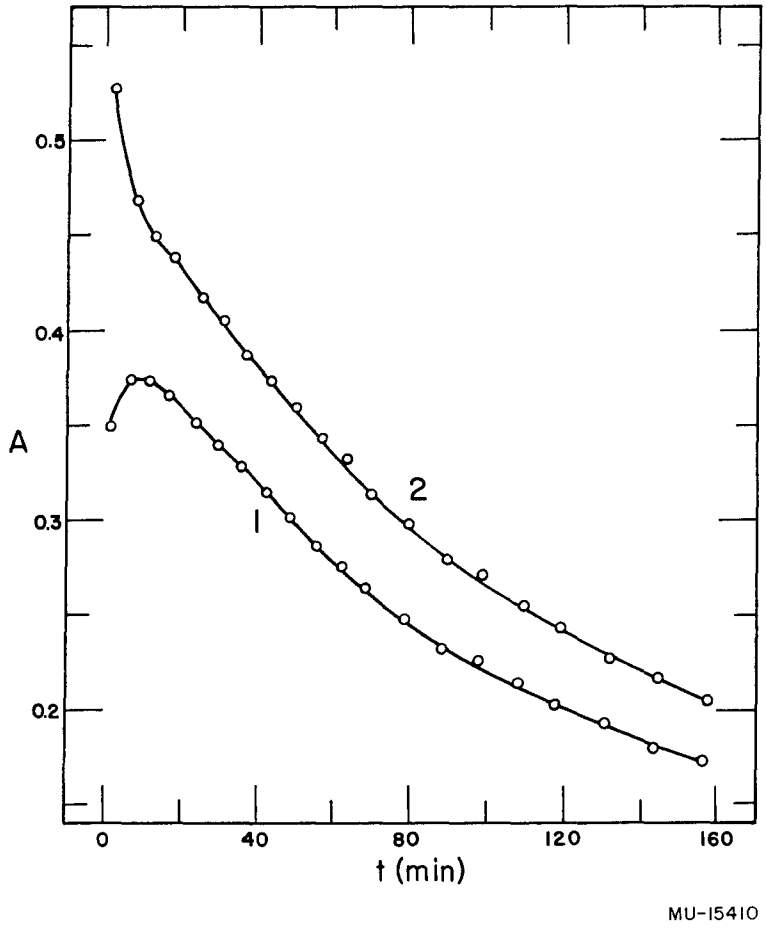

Fig. 8. The absorbance-time curve of Experiment IV-A-2-C of Table V. Curve 1 : λ = 400.6 mμ ; Curve 2 : λ = 320.1 mμ.

The syringe was carefully lubricated with Kel-F #90 grease before each run. To prevent contamination of the reagent by grease in the syringe, the latter was lubricated with as little grease as possible only in the part higher than the 2.5-ml mark. However, it was found that too thin a layer of grease caused the formation of bubbles during the mixing and thus gave erroneous spectrophotometric results.

No reaction between the #16 stainless steel hypodermic needle and the basic hypochlorite solution could be detected spectrophotometrically. This was tested by immersing the stainless steel hypodermic needle in a basic ClO^- solution (0.500 M OH^- and 0.010 M of ClO^-) for over an hour. The absorption spectrum of the ClO^- solution was examined before and after the 1-hr immersion. No difference in the shapes of the absorption curve or the absorbances was found. Therefore the reaction between ClO^- and the stainless steel hypodermic needle was negligible.

(2) Experimental Procedure

Eight ml of solution with the desired concentrations of OH^- and ClO^- were pipetted into the 2.15-cm cell which had been previously air-dried. The cell with its contents was placed in the cell compartment of the Cary recording spectrophotometer. The wavelength scale was set at 400.6 mμ, the room was darkened, the cover of the cell compartment was removed, and the absorbance of the basic ClO^- solution was measured for use as a blank for the later calculation. Basic iodide solution with the desired concentration of iodide and the same hydroxide concentration as that of the solution in the cell was carefully introduced into the hypodermic syringe through the needle. When it was certain that there were no bubbles in the syringe, the volume of this basic iodide solution was adjusted to the 2.0-ml mark. With the cell set

in the light path and with the Cary spectrophotometer's master switch turned on (i.e. the switches controlling the slit, pen, and chart were all on), the basic iodide solution in the syringe was injected into the cell manually. The syringe was held in such a position that the needle was just below the surface of the solution in the cell and barely out of the light path. The measurement of absorbance was carried on as a function of time usually over an hour.

The zero time was taken as the time at which the absorbance on the spectrophotometer chart started to rise. The times of other points on the absorption curve were calculated on the basis of the running speed of the chart.

For experiments to investigate the hydroxide dependence of the rate, NaCl was used to keep the ionic strength at 1.00 M, with chloride solution added to both the syringe and the cell solutions.

No effect of reversing the order of mixing was detected by injecting basic ClO^- solution into a basic iodide solution in the cell.

(C) Results and Calculation of the Rate Constant for a Typical Experiment

The absorption curves shown on the Cary spectrophotometer chart from the runs made by the injection method described above were very smooth curves. They started from a point with an absorbance equal to that of the blank solution, gradually reached a certain value of absorbance, and remained constant for a period of time before decreasing again.

Figure 9 shows the plot of absorbance versus time for Experiment IV-K-1-b. Here k is defined as the rate constant of the formation of IO^- from I^- and ClO^-. The calculation of k for Experiment IV-k-1-b is listed in Table VI. The first column records the time in seconds. The

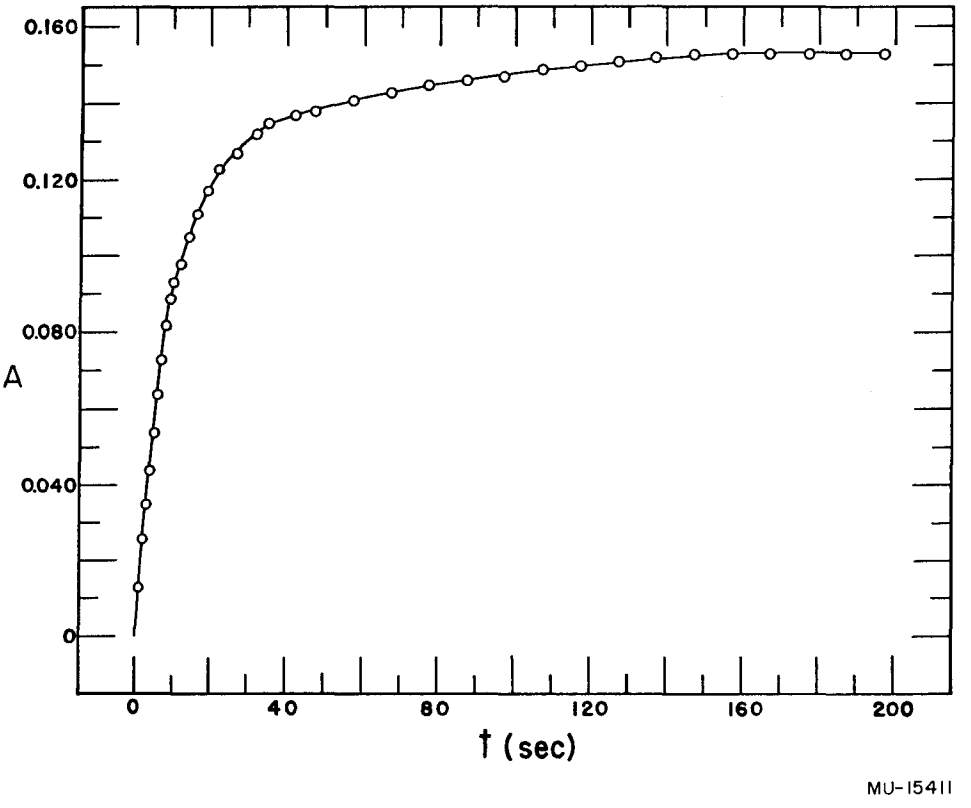

Fig. 9. The absorbance-time curve of Experiment IV-K-1-b. λ = 400.6 mμ.

Table VI

Calculation of k for a typical experiment

(Experiment IV-K-1-b of Table VII)*

Time (sec)	A	(IO^-) ($\times 10^3$ M)	$(I^-) = (OCl^-)$ ($\times 10^3$ M)	$d(IO^-)/dt$ ($\times 10^4$)	k (M^{-1} sec^{-1})
2.0	0.026	0.314	1.686	1.752	61.7
3.0	0.035	0.423	1.577	1.493	60.1
4.0	0.044	0.531	1.469	1.257	58.4
5.0	0.054	0.652	1.348	1.118	61.5
6.0	0.064	0.773	1.227	0.920	61.2
8.0	0.082	0.991	1.009	0.619	60.9
14.0	0.105	1.269	0.731	0.326	60.6

*$(I^-)_{in} = 2.00 \times 10^{-3}$ M

$(ClO^-)_{in} = 2.00 \times 10^{-3}$ M

$(OH^-)_{in} = 1.00$ M

second column represents the observed absorbance with correction for the blank. The third column gives the concentration of IO^- in moles per liter calculated from the absorbance by the use of

$$(IO^-) = A/b\ \epsilon_{IO^-}^{400.6}$$

where $\epsilon_{IO^-}^{400.6}$ is the molar absorptivity of IO^- at 400.6 mμ, and b is the cell length. During the period of first 14 sec, which was the time interval used in Table VI to calculate k, the rate of disproportionation of IO^- was negligible. The values of the iodide concentrations in the fourth column were obtained by subtracting the IO^- concentrations from the initial iodide concentration, and were assumed to be equal to that of ClO^-. From the slope of the A-t curve in Fig. 9 at time t, the value of $d(IO^-)/dt$ was calculated and reported as such in the fifth column. The values of the rate constant k in the last column were defined as

$$k = \frac{1}{(I^-)(ClO^-)} \quad \frac{d(IO^-)}{dt} \ .$$

The uncertainty of the average value of k was estimated from all possible experimental sources of error as well as from the uncertainty in measuring the slope. The uncertainty of the recording of zero time and its effect on the calculation of k should be pointed out. The time required for complete mixing is unknown. Therefore the zero time, which was taken as the time when the absorbance on the spectrophotometer chart started to rise, might not be the true zero time if the mixing is not instantaneous. Because it is very hard to tell what the true zero time is, the values of k of all experiments using the injection method were calculated by measuring the slopes of the A-t curve at individual times in order to minimize effects of the accuracy of zero time on k.

The values of k from other experiments with different initial concentrations of ClO^-, I^- and OH^- are listed in Table VII. All the headings in the latter are self-explanatory.

Table VII

Rate data on ClO^- - I^- reaction from injection method

Exp't. No.	$(ClO^-)_{in}$ (x 10^3 M)	$(I^-)_{in}$ (x 10^3 M)	$(OH^-)_{in}$ (M)	$(Cl^-)_{in}$ (M)	k (M^{-1} sec^{-1})	k x$(OH^-)_{in}$ (sec^{-1})
IV-G-1-d	4.00	2.00	1.00	0.004	60.3 ± 5	60.3 ± 5
IV-J-1-c	2.00	4.00	1.00	0.002	62.7 ± 5	62.7 ± 5
IV-K-1-b	2.00	2.00	1.00	0.002	60.6 ± 5	60.6 ± 5
IV-K-2-a	2.00	2.00	0.500	0.502	116 ± 10	58.0 ± 5
IV-K-3-c	2.00	2.00	0.250	0.752	234 ± 20	58.5 ± 5

(D) Acid Dependence

As shown in the last column of Table VII, the values of $k \times (OH^-)_{in}$ of all experiments using the injection method remained constant within the experimental error. This indicates that the rate of the formation of IO^- from ClO^- and I^- in alkaline solution is inversely proportional to the hydroxide concentration.

(E) Rate Law

As indicated in Table VII, in 1.00 M OH^- solution, when the ratios of the initial concentration of ClO^- to that of I^- was changed from 1 : 1 to 2 : 1 or 1 : 2, the rate constant, which was calculated by assuming $k = \frac{d(IO^-)}{dt} \times \frac{1}{(I^-)(ClO^-)}$, remained constant within the experimental error. Therefore the rate of formation of hypoiodite from hypochlorite and iodide in 1.00 M hydroxide solution is first-order dependent on both hypochlorite and iodide concentrations. Moreover, as described above, the rate was found to be inversely proportional to the hydroxide concentration. As a consequence the rate law can be expressed as

$$\frac{d(IO^-)}{dt} = \frac{k(I^-)(ClO^-)}{(OH^-)},$$

where k has the value 61 ± 3 sec^{-1} at an ionic strength of 1.00 M at $25^{\circ}C$.

(F) Discussion

Many reactions between ions of like charge are catalyzed by ions of opposite charge. Proton catalysis of reactions between anions, like the one studied here, might be ascribed to this phenomenon. Two mechanisms with the reaction between HOCl and I^- as the determining step were considered to be possible for the formation of IO^- from I^- and ClO^-.

The first mechanism can be expressed as follows:

$$ClO^- + H_2O \rightleftharpoons HOCl + OH^- \quad \text{(rapid equilibrium)},$$

$$HOCl + I^- \xrightarrow{k} HOI + Cl^- \quad \text{(rate determining)},$$

$$HOI + OH^- \rightleftharpoons IO^- + H_2O \quad \text{(fast)}.$$

In this mechanism I^- attacks the OH of HOCl so that oxygen transfer occurs. This mechanism is analogous to the mechanism suggested by Farkas, Lewin, and Bloch for the formation of BrO^- from ClO^- and Br^-.[11] The latter reaction was also discussed recently by Anbar and Taube.[12]

The other mechanism, which includes the attack of I^- on Cl of HOCl, might be

$$ClO^- + H_2O \rightleftharpoons HOCl + OH^- \quad \text{(rapid equilibrium)},$$

$$HOCl + I^- \xrightarrow{k} ICl + OH^- \quad \text{(rate determining)},$$

$$ICl + 2OH^- \rightleftharpoons IO^- + Cl^- + H_2O \quad \text{(fast)}.$$

The rate-determining step could be thought of as a nucleophilic displacement of hydroxyl ion by the I^-.[13]

In view of the composition of the activated complex $(HOClI)^-$ of the reaction studied, the only reasonable place for the proton in the activated complex is on oxygen.[12] According to either mechanism, the role of H^+ is to labilize the oxygen-chlorine bond. It is hard to tell which one of the two mechanisms would be more favorable. Anbar and Taube pointed out from their results of the rate of exchange of oxygen between BrO^- and water in alkaline solution that the rates of attack of Br in HOBr by Br^- and Cl^- are about equal.[12] However the specific rate (1.77×10^5 $\underline{M}^{-1}$ min^{-1} at zero ionic strength) for Br^- reacting with HOCl is almost 20 times that for Cl^- substituting on Cl in HOCl.[11,12]

Because of this relatively higher rate for Br^- reacting with HOCl, they suggested that it is more likely that bromine attacks the oxygen of HOCl. The specific rate (k) for I^- reacting with HOCl can be calculated from our investigation by finding the difference between

$$H_2O \overset{K_{H_2O}}{\rightleftharpoons} H^+ + OH^- \quad (K_{H_2O} = 10^{-14}) \qquad (2)$$

and

$$HOCl \overset{K_{HOCl}}{\rightleftharpoons} H^+ + ClO^- \quad (K_{HOCl} = 3.44 \times 10^{-8}), \qquad (3)^{14}$$

$$ClO^- + H_2O \overset{K'}{\rightleftharpoons} HOCl + OH^-$$

which is (Eq. (2) - Eq. (3)), where $K' = (HOCl)(OH^-)/(ClO^-) = 2.91 \times 10^{-7}$. From the rate law of the formation of IO^- from I^- and ClO^-, one obtains

$$-\frac{d(ClO^-)}{dt} = \frac{61\,(I^-)(ClO^-)}{(OH^-)} = k(HOCl)(I^-).$$

Therefore $k = 61/K' = 2.10 \times 10^8\ \underline{M}^{-1}\ sec^{-1} = 1.26 \times 10^{10}\ \underline{M}^{-1}\ min^{-1}$. By comparing the value of k with the corresponding result for Br^- from Farkas, Lewin, and Bloch,[11] one concludes that I^- reacts with HOCl about 7×10^4 times faster than does Br^- (i.e. almost 10^6 times faster than does Cl^-). If one accepts the above-mentioned suggestion made by Anbar and Taube,[12] this much higher rate for I^- reacting with HOCl would strongly indicate that iodine attacks the oxygen of HOCl.

VI. STUDIES OF THE EQUILIBRIA BETWEEN IO^-, I_3^-, I^-, I_2OH^-, and $I_2O^=$

(A) Other Species

(1) The Presence of Triiodide Ion

In addition to the species later identified as IO^-, it was evident from the spectra that other species were sometimes present. During the investigation of the rate of disproportionation of IO^-, it was observed spectrophotometrically that when the initial hydroxide concentration was lower than 1 M and the iodide concentration was equal to or higher than 0.1 M, an appreciable amount of I_3^- was present. The presence of I_3^- in some cases could be detected by just looking at the absorption curve from the Cary spectrophotometer chart. For example, under the condition of $(I^-)_{in} = 0.1020$ M, $(ClO^-)_{in} = 2.000 \times 10^{-3}$ M, and $(OH^-)_{in} = 0.1000$ M (Experiment II-H-5), the characteristic absorption peak of I_3^- at 353.0 mμ was shown very clearly on the chart.[8] Therefore, it seemed worthwhile to study the following equilibrium:

$$IO^- + 2I^- + H_2O \underset{}{\overset{K_2}{\rightleftharpoons}} I_3^- + 2OH^-, \qquad (4)$$

where $K_2 = (I_3^-)(OH^-)^2/(IO^-)(I^-)^2$.

When hypoiodite ion was produced with an initial iodide concentration of 1.0002 M, hydroxide concentration of 0.0500 M, and hypochlorite concentration of 2.00×10^{-4} M, the majority of the absorption was due to I_3^-. However the ratio of the absorbances at zero time at 360.5 mμ and 400.6 mμ was found to be 3.63, which is smaller than the value calculated from the known molar absorptivities of I_3^-.[8] Therefore the absorption spectrum of pure I_3^- was measured in a 1.000 M I^- solution, and it was found that the value of $\epsilon_{I_3^-}^{360.5} / \epsilon_{I_3^-}^{400.6}$ was equal to 3.62. As a consequence, the I_3^- absorption spectrum was studied as a function of iodide concentration

as reported in Part IV, and molar absorptivities were obtained as a function of the I^- concentration.

(2) The Presence of I_2OH^-

The first attempt to study the equilibrium constant K_2 of Eq. (4) was made under the assumption that +1 iodine and I_3^- were the only two iodine species present as the product of the reaction between I^- and ClO^-. However, when the dependences of the equilibrium between +1 iodine and I_3^- on the concentrations of OH^- as well as I^- were studied spectrophotometrically, it was found that the data could not be fitted assuming the +1 iodine species to be IO^-. Some preliminary results indicated that the ratio of I_3^- to +1 iodine might depend on the inverse first power of the hydroxide concentration and the square of the iodide concentration, corresponding to the equilibrium:

$$HOI + 2I^- = I_3^- + OH^- \quad .$$

On the basis of this assumption, the hydrolysis constant of iodine could be calculated by adding algebraically Eqs. (5), (6), and (2),

$$I_3^- + OH^- = HOI + 2I^- \quad , \qquad (5)$$

$$I_2 + I^- = I_3^- \quad , \qquad (6)$$

$$H_2O = H^+ + OH^- \quad . \qquad (2)$$

The summation is

$$I_2 + H_2O = HOI + I^- + H^+ \quad . \qquad (7)$$

The value for the hydrolysis constant thus obtained was about one hundred times greater than those reported in the literature,[2,15,16,17] thus ruling out HOI as the principal +1 iodine species in 1 M hydroxide. Finally it was concluded that the assumption of only two iodine species in addition to I^- was erroneous.

As a second approach, spectrophotometric runs over a considerably larger range of I^- and OH^- concentrations were done. The experimental procedure and the method for getting the values of the effective molar absorptivities at 400.6 mμ, 360.5 mμ, 320.1 mμ and 289.9 mμ were the same as described in Part IV. The results are listed in Table VIII with $(I^-)_o$ and $(OH^-)_o$ representing the concentrations of I^- and OH^- respectively after mixing. The values of $\bar{\epsilon}$ were plotted against the values of $(I^-)_o/(OH^-)_o$ on logarithmic paper. The solid circles represent experiments with the initial hydroxide concentrations equal to 0.1000 M, and the open circles are experiments with concentrations other than 0.1000 M. (For reasons which will be clear later, the curves in the region where the value of $(I^-)_o/(OH^-)_o$ varies from 0.01 to 10 were drawn through the solid circles.) As shown in Fig. 10 and Fig. 11, quite smooth curves were obtained. This indicates that the effective molar absorptivity was some function of $(I^-)_o/(OH^-)_o$. From Eq. (4) the equilibrium ratio of (I_3^-) to (IO^-) is second-order dependent on the function $(I^-)/(OH^-)$. Quite naturally the existence of another species that would give a first-order dependence on $(I^-)/(OH^-)$ was considered - this is I_2OH^-. The equilibrium between IO^- and I_2OH^- can be expressed as follows:

$$IO^- + I^- + H_2O \underset{\longleftarrow}{\xrightarrow{K_1}} I_2OH^- + OH^- \qquad (8)$$

where $K_1 = (I_2OH^-)(OH^-)/(IO^-)(I^-)$.

It was readily shown that IO^- and I_3^- alone or I_2OH^- and I_3^- alone would not account for the spectral data. By the method which will be explained later, it was found that the assumption of the presence of IO^-, I_3^-, and I_2OH^- fitted the spectral data very well when the hydroxide concentration was held constant. Deviations from the fit were found at

Table VIII

Effective molar absorptivities

Exp't. No.	$(OH^-)_{in}$ (M)	$(I^-)_{in}$ ($\times 10^3$ M)	$(ClO^-)_{in}$ ($\times 10^3$ M)	(ClO_4^-) (M)	$(I^-)_o/(OH^-)_o$	$\bar{\epsilon}^{400.6}$	$\bar{\epsilon}^{360.5}$	$\bar{\epsilon}^{320.1}$	$\bar{\epsilon}^{289.9}$
III-A-3	1.000	2.500	1.803	-	6.97×10^{-4}	37.7	57.4	47.4	129.5
III-P-1	1.000	10.00	9.017	-	9.83×10^{-4}	38.8	58.8	49.2	141.0
III-A-4	1.000	4.000	1.803	-	2.197×10^{-3}	37.6	58.0	48.0	-
III-G-5	1.004	3.141	*1.803	-	6.744×10^{-3}	38.3	56.0	46.8	132.2
III-H-1	1.000	8.950	1.803	-	7.147×10^{-3}	40.5	61.0	48.7	140.0
III-G-4	1.004	3.655	*1.800	-	7.252×10^{-3}	38.0	59.0	51.9	143.8
III-G-3	1.004	3.676	*1.810	-	7.293×10^{-3}	38.2	56.8	46.9	136.3
II-R-2-a	0.1000	2.000	1.000	-	1.000×10^{-2}	37.0	55.9	46.1	135.0
III-L-1	0.2040	3.147	*1.803	0.8000	3.370×10^{-2}	37.3	59.5	48.8	138.3
II-X-1	0.1000	12.00	2.000	-	0.1000	40.5	65.4	56.0	169.8
IV-M-1	0.1000	12.00	2.000	0.9900	0.1000	39.4	64.9	55.7	167.1
II-X-3	1.000	102.0	2.000	-	0.1000	39.7	69.7	59.6	206
II-H-6	0.5000	102.0	2.000	-	0.2000	41.6	75.2	67.1	234
IV-R-2	1.000	349.0	1.000	-	0.3480	47.0	103.8	95.8	410
II-H-4	0.2000	102.0	2.000	0.3000	0.5000	48.3	110.3	96.0	334
II-G-1	0.1000	52.00	2.000	-	0.5000	52.7	115.6	100.7	323
IV-P-1	0.5000	500.2	0.2000	-	1.000	74.5	220	190.5	705
II-H-5	0.1000	102.0	2.000	0.4000	1.000	73.2	204	163.5	550
IV-N-2	0.5000	1000.2	0.2000	-	2.000	147.5	467	354	1292
II-H-7	0.0500	102.0	2.000	0.4500	2.000	140	465	349	1112
II-J-1	0.1000	500.2	0.2000	-	5.000	515	1935	1265	3.53×10^3
II-K-1	0.1000	500.3	*0.2000	-	5.027	540	1995	1330	3.69×10^3
II-Y-1	0.2000	1000.2	0.2000	-	5.000	527	1847	1230	3.36×10^3
II-U-1	0.1000	1000.2	0.2000	-	10.00	1375	5.00×10^3	3.07×10^3	7.83×10^3
II-L-2	0.0500	1000.2	0.2000	-	20.00	2.71×10^3	9.81×10^3	5.93×10^3	1.418×10^4

* I_3^- was used as the starting material

higher hydroxide concentrations. Therefore the presence of a fourth species, which was in equilibrium with hydroxide, was apparent.

(3) Dependence of Effective Molar Absorptivity on Hydroxide Concentration and Presence of $I_2O^=$

Under the assumption of the presence of IO^-, I_3^-, and I_2OH^-, the relation

$$A_{obs} = A_{IO^-} + A_{I_3^-} + A_{I_2OH^-} \qquad (9)$$

should hold, where A represents absorbance. From Eq. (9) and the two equilibrium constants K_1 and K_2 of Eq. (8) and Eq. (4), Eq. (10) can be easily derived:

$$\bar{\epsilon} = \frac{\epsilon_{IO^-} + K_1 \epsilon_{I_2OH^-} [(I^-)/(OH^-)] + K_2 \epsilon_{I_3^-} [(I^-)^2/(OH^-)^2]}{1 + K_1(I^-)/(OH^-) + K_2(I^-)^2/(OH^-)^2} \qquad (10)$$

From Eq. (10), experiments in Table VIII having the same values of $(I^-)_o/(OH^-)_o$ should give equal values of $\bar{\epsilon}$ if IO^-, I_3^-, and I_2OH^- are the three correct species. In other words, at each of the four wavelengths in Fig. 10 and 11, the values of the abscissas of the points with the same ordinate values should agree within experimental error, if the above assumption holds. As mentioned earlier, in the region of $(I^-)_o/(OH^-)_o$ from 0.01 to 10, the curves were drawn through the points for experiments with 0.100 M initial hydroxide concentration. As shown in these two figures, at 400.6 mμ very small deviations were found between the $\bar{\epsilon}$ values of 0.100 M OH^- and those of higher hydroxide concentrations. However at 289.9 mμ a pronounced deviation between experiments at different hydroxide concentrations was observed in the region where the value of $(I^-)_o/(OH^-)_o$ ranged from 3.5×10^{-2} to 2. As to the two intermediate wavelengths (i.e. 360.5 mμ and 320.1 mμ), the effect of hydroxide

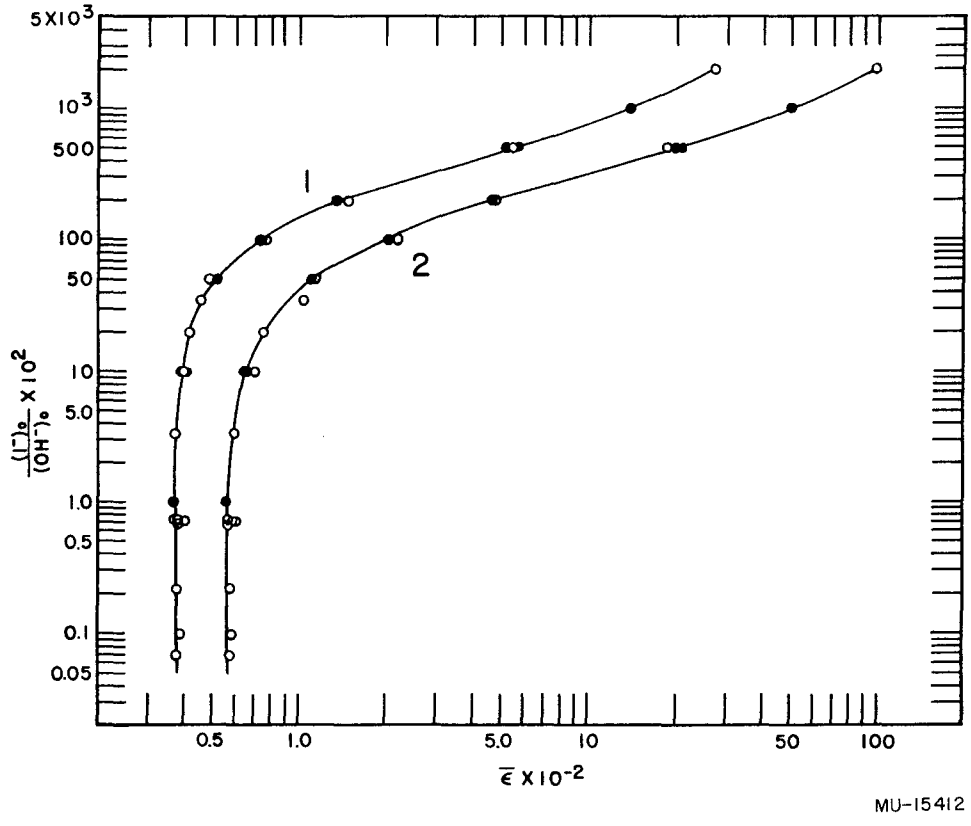

Fig. 10. Plot of $(I^-)_0/(OH^-)_0$ vs $\bar{\epsilon}$.
Curve 1 : λ = 400.6 mμ ; Curve 2 : λ = 360.5 mμ.

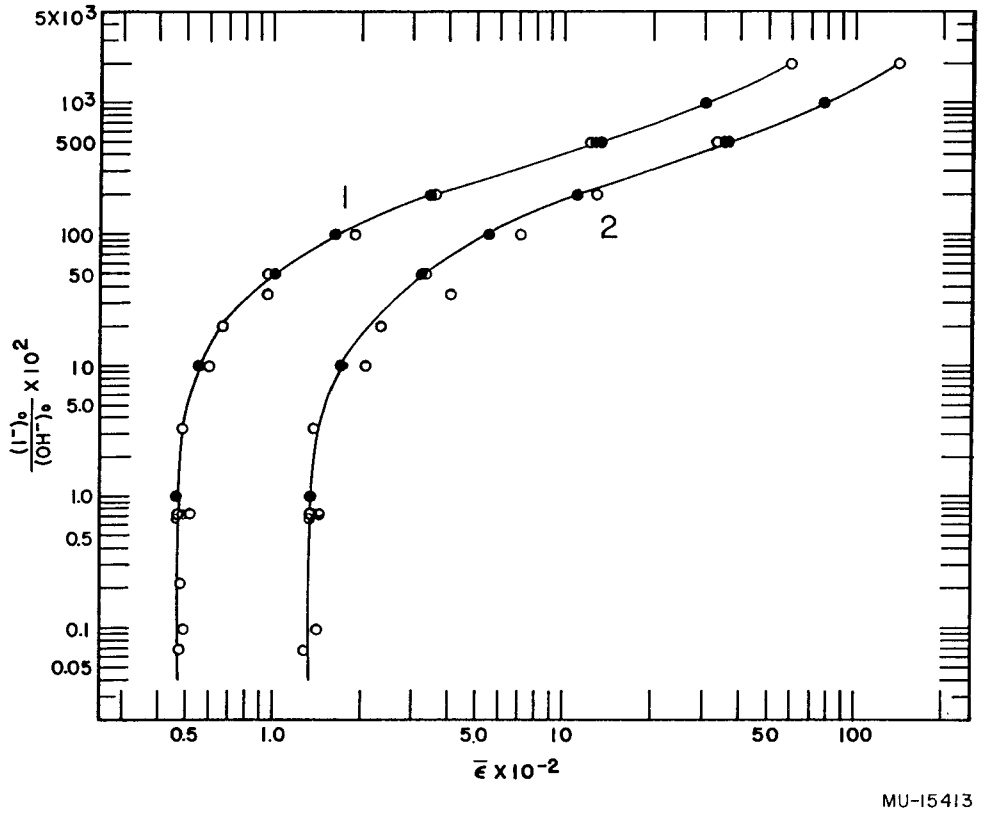

Fig. 11. Plot of $(I^-)_0/(OH^-)_0$ vs $\bar{\epsilon}$.
Curve 1 : λ = 320.1 mμ ; Curve 2 : λ = 289.9 mμ.

concentration on $\bar{\epsilon}$ was smaller than that at 289.9 mμ but greater than that at 400.6 mμ. This result indicates that at least one of the three species (i.e. IO^-, I_3^-, and I_2OH^-) is tied up by hydroxide ion, and that the new species absorbs strongly at 289.9 mμ. The species that is tied up by hydroxide could not be IO^-, because the molar absorptivity determined for IO^- at very low ratios of $(I^-)_o/(OH^-)_o$ is the same for 0.1 M and 1 M OH^- solutions and is in agreement with the limiting value of Figs. 10 and 11 at low $(I^-)_o/(OH^-)_o$. Similarly I_3^- was considered not likely to be the species that was tied up by OH^- because the deviation of $\bar{\epsilon}$ caused by different hydroxide concentration between experiments with the same $(I^-)_o/(OH^-)_o$ was found to be negligible in the region of high ratios of $(I^-)_o/(OH^-)_o$, where the majority of the absorption was due to I_3^-. In Fig. 11, one notices that the region where the deviation was observed was actually the region where I_2OH^- was supposed to be present in appreciable concentration. This gives evidence that the species that was tied up by OH^- was I_2OH^-.

From the above considerations, it was believed that the fourth species that causes the difference in $\bar{\epsilon}$ of two experiments with the same $(I^-)_o/(OH^-)_o$ but different initial OH^- concentrations is $I_2O^=$, or

$$I_2OH^- + OH^- \underset{}{\overset{K_3}{\rightleftharpoons}} I_2O^= + H_2O \quad .$$

However, in order to eliminate the possibility that the fourth species was some ion other than $I_2O^=$, attempts were made to find the formula of the fourth ion in a more general way. One may write the general equation:

$$IO^- + xOH^- + yI^- \overset{Q_4}{\rightleftharpoons} \text{new species}$$

where $Q_4 = (\text{new species})/(IO^-)(OH^-)^x(I^-)^y$. For the 289.9-mμ curve from Fig. 11, it may be seen that changing the initial IO^- concentration has

little or no effect on the deviations of $\bar{\epsilon}$ from the curve for the 0.100 M OH^- solutions, thus leading to the conclusion that the new species contains one IO^-. This may be seen best in the values for Experiments IV-R-2 and IV-P-1 with $\bar{\epsilon}$ values at 289.9 mμ of 410 and 705, respectively. The deviations from the curve do not differ by anywhere near the five-fold change in IO^- concentration. A ten-fold change in IO^- concentration between Experiment IV-R-2 and an experiment not reported because of the uncertainty in the extrapolated absorbance leads to the same conclusion.

With four species contributing to the light absorption, Eq. (10) becomes

$$\bar{\epsilon} = \frac{\epsilon_{IO^-} + K_1\epsilon_{I_2OH^-}(I^-)/(OH^-) + K_2\epsilon_{I_3^-}(I^-)^2/(OH^-)^2 + Q_4\epsilon_4(OH^-)^x(I^-)^y}{1 + K_1(I^-)/(OH^-) + K_2(I^-)^2/(OH^-)^2 + Q_4(OH^-)^x(I^-)^y}, \quad (11)$$

with ϵ_4 representing the molar absorptivity of the fourth species. In order to determine the values of x and y, the values of K_1, K_2, and $\epsilon_{I_2OH^-}$ must be known first. As an approximation, it was assumed that when the hydroxide concentration was equal to or smaller than 0.100 M, the presence of $I_2O^=$ would not be appreciable, i.e. the effect of $I_2O^=$ on the light absorption was small enough to be negligible. Therefore Eq. (10) could be used and was rearranged to

$$\frac{\bar{\epsilon} - \epsilon_{IO^-} + \bar{\epsilon}K_1(I^-)/(OH^-)}{(I^-)/(OH^-)} = K_1\epsilon_{I_2OH^-} + K_2(\epsilon_{I_3^-} - \bar{\epsilon})(I^-)/(OH^-). \quad (12)$$

In Eq. (12), K_1, K_2, and $\epsilon_{I_2OH^-}$ are unknown. A graphical method was used to obtain the constants. If K_1 is known, the value of the left side of the equation is fixed by the experimental data, while the right side is known except for $\epsilon_{I_2OH^-}$ and K_2. Thus the equation reduces to the form Y = a + bX where a and b are constants and X is $(\epsilon_{I_3^-} - \bar{\epsilon})(I^-)/(OH^-)$.

The fit of the data to this equation was tested by a log-log plot of the left side (Y) of Eq. (12) versus X. The fit was tested by superimposing a master curve from the equation $Y_o = 1 + X_o$ plotted on transparent graph paper of the same scale. Horizontal and vertical movement of the curves relative to each other was used until the best fit was obtained. The positioning of the two scales relative to each other yields $K_1\epsilon_{I_2OH^-}$ and K_2. Becuase the value of K_1 was not known, it was necessary to make a series of plots of the experimental data with different assumed values of K_1 to find the value of this parameter which best fitted the data. Values of K_1 ranging from 0.4 to 0.04 were tried. It was found that with $K_1 = 0.115$ the best fit of the master curve was obtained. The $\bar{\epsilon}$ values of four wavelengths, namely 400.6 mμ, 360.5 mμ, 320.1 mμ, and 289.9 mμ, were used for the calculations. Because this kind of calculation and plot with further refinements will appear later (Figs. 13 to 16), no figure will be given here. The $\epsilon_{I_3^-}$ used in the calculation is the value at the iodide concentration of the experiment.

From Eq. (12), the ordinate limit of the curve is $K_1\epsilon_{I_2OH^-}$. Because the best value of K_1 was found as 0.115, $\epsilon_{I_2OH^-}$ could thus be calculated. The abscissa on the master plot is $K_2(\epsilon_{I_3^-} - \bar{\epsilon})[(I^-)/(OH^-)]/K_1\epsilon_{I_2OH^-}$ and that on the plot of data is $(\epsilon_{I_3^-} - \bar{\epsilon})(I^-)/(OH^-)$; therefore, when the master plot and the plot of data were superimposed, the abscissa value of the latter which corresponds to $X_o = 1$ on the former should satisfy the equation,

$$K_2/K_1\epsilon_{I_2OH^-} = 1/\text{abscissa value on the plot of data at } X_o = 1. \qquad (13)$$

Since $K_1\epsilon_{I_2OH^-}$ is the ordinate limit as mentioned above, therefore

$$K_2 = \frac{\text{(ordinate limit on the plot of data)}}{\text{(abscissa value on the plot of data at } X_o = 1)}. \qquad (14)$$

The average K_2 value obtained from the curves at 400.6 mμ, 360.5 mμ, and 320.1 mμ as well as 289.9 mμ was 4.5×10^{-3}.

By knowing the values of K_1, K_2, and $\epsilon_{I_2OH^-}$, one can go back to Eq. (11) and attempt to get the value of x and y. For any pair of experiments of Table VIII that had the same $(I^-)_o/(OH^-)_o$ but different initial iodide and hydroxide concentrations, one can designate the experiment with higher (OH^-) as No. 1 and the one with lower hydroxide as No. 2. The results of both experiments then can be substituted into Eq. (11) independently as follows:

$$\bar{\epsilon}_1 = \frac{\epsilon_{IO^-} + K_1 \epsilon_{I_2OH^-} \frac{(I^-)}{(OH^-)} + K_2 \epsilon_{I_3^-} \frac{(I^-)^2}{(OH^-)^2} + Q_4 \epsilon_4 (OH^-)_1^x (I^-)_1^y}{1 + K_1 \frac{(I^-)}{(OH^-)} + K_2 \frac{(I^-)^2}{(OH^-)^2} + Q_4 (OH^-)_1^x (I^-)_1^y} \quad (15)$$

$$\bar{\epsilon}_2 = \frac{\epsilon_{IO^-} + K_1 \epsilon_{I_2OH^-} \frac{(I^-)}{(OH^-)} + K_2 \epsilon_{I_3^-} \frac{(I^-)^2}{(OH^-)^2} + Q_4 \epsilon_4 (OH^-)_2^x (I^-)_2^y}{1 + K_1 \frac{(I^-)}{(OH^-)} + K_2 \frac{(I^-)^2}{(OH^-)^2} + Q_4 (OH^-)_2^x (I^-)_2^y} \quad (16)$$

where the newly added subscripts 1 and 2 refer to experiments 1 and 2 respectively. From Equations (15) and (16), we have

$$(\bar{\epsilon}_1 - \bar{\epsilon}_2)\left[1 + \frac{K_1(I^-)}{(OH^-)} + \frac{K_2(I^-)^2}{(OH^-)^2} + Q_4(OH^-)_1^x(I^-)_1^y\right]\left[1 + \frac{K_1(I^-)}{(OH^-)} + \frac{K_2(I^-)^2}{(OH^-)^2}\right.$$

$$\left. + Q_4(OH^-)_2^x(I^-)_2^y\right] = Q_4\left[\epsilon_{IO^-} + K_1\,\epsilon_{I_2OH^-}\,\frac{(I^-)}{(OH^-)}\right]\left[(OH^-)_2^x(I^-)_2^y - (OH^-)_1^x(I^-)_1^y\right]$$

$$+ \frac{K_2(I^-)^2}{(OH^-)^2}(\epsilon_{I_3^-} - \epsilon_{I_3^-})\left[1 + \frac{K_1(I^-)}{(OH^-)} + \frac{K_2(I^-)^2}{(OH^-)^2}\right] + K_2Q_4\,\frac{(I^-)^2}{(OH^-)^2}\;x$$

$$\left[\epsilon_{I_3^-}(OH^-)_2^x(I^-)_2^y - \epsilon_{I_3^-}(OH^-)_1^x(I^-)_1^y\right] + \epsilon_4Q_4\left[(OH^-)_1^x(I^-)_1^y - (OH^-)_2^x(I^-)_2^y\right]\;x$$

$$\left[1 + \frac{K_1(I^-)}{(OH^-)} + \frac{K_2(I^-)^2}{(OH^-)^2}\right] \qquad . \qquad (17)$$

Eq. (17) can be rearranged as follows:

$$(\bar{\epsilon}_1-\bar{\epsilon}_2)\left[1 + \frac{K_1(I^-)}{(OH^-)} + \frac{K_2(I^-)^2}{(OH^-)^2} + Q_4(OH^-)_1^x(I^-)_1^y\right]\left[1 + \frac{K_1(I^-)}{(OH^-)} + \frac{K_2(I^-)^2}{(OH^-)^2} + Q_4(OH^-)_2^x(I^-)_2^y\right]$$

$$\left[(OH^-)_1^x(I^-)_1^y - (OH^-)_2^x(I^-)_2^y\right]\left[1 + \frac{K_1(I^-)}{(OH^-)} + \frac{K_2(I^-)^2}{(OH^-)^2}\right]$$

$$+ \frac{\dfrac{K_2(I^-)^2}{(OH^-)^2}\,(\epsilon_{I_3^-} - \epsilon_{I_3^-})}{\left[(OH^-)_1^x(I^-)_1^y - (OH^-)_2^x(I^-)_2^y\right]} = Q_4\epsilon_4$$

$$-Q_4\left\{\frac{\left[\epsilon_{IO^-} + \epsilon_{I_2OH^-}\,\dfrac{K_1(I^-)}{(OH^-)}\right] - \dfrac{\dfrac{K_2(I^-)^2}{(OH^-)^2}\left[\epsilon_{I_3^-}(OH^-)_2^x(I^-)_2^y - \epsilon_{I_3^-}(OH^-)_1^x(I^-)_1^y\right]}{(OH^-)_1^x(I^-)_1^y - (OH^-)_2^x(I^-)_2^y}}{1 + K_1\,\dfrac{(I^-)}{(OH^-)} + K_2\,\dfrac{(I^-)^2}{(OH^-)^2}}\right\} \qquad (18)$$

In Eq. (18) all quantities are known - at least approximately - except Q_4, ϵ_4, x, and y. From Eq. (18), if experimental values of the two terms on the left side of the equation are plotted against the total value within the braces on the right side, one should get a straight line with slope equal to Q_4 and intercept equal to $Q_4\epsilon_4$, provided the correct values of x and y have been chosen. On the other hand, the plot would not be a straight line if the wrong species were assumed. In making this kind of plot, actually a method of successive approximation has to be used because the value of Q_4, which is included in one of the terms on the left side of the equation, is initially not known. The first approximation was carried out by neglecting the terms containing Q_4. Then the slope of that line was used for the value of Q_4 in the second approximation, the calculation was carried out as above until two successive approximations gave the same values of Q_4. Different combinations of the values of x and y, each ranging from -2 to +2, were tried with the data at 289.9 mμ of the eight pairs of experiments in Table VIII. (The values of $\bar{\epsilon}_2$ in the two pairs containing experiments II-H-6 and IV-R-2 were obtained from the curves in Fig. 11.) It was concluded that there would be no possible solutions of x and y with $y < -1$ since this would correspond to a negative number of iodine atoms in the new species. The results as shown in Table IX indicated that only when $x = 0$, $y = 1$ could a straight line be drawn within the experimental error. In the case where $x = 1$ and $y = 1$, it is possible that the plot could be a straight line, however it would not fit the points as well as when $x = 0$ and $y = 1$. All the other plots were not straight lines. The straight line in the case of $x = 0$ and $y = 1$, which gave a value of $Q_4 = 0.11$, will not be shown here since a similar line

Table IX

The formula of the fourth species			
x*	y*	Formula of the fourth species (i.e. besides IO^-, I_3^- and I_2OH^-)	Remarks about the plot
-2	2	I_3^-	-
-1	-1	$H_3O_2^+$ or HO^+	thermodynamically impossible
-1	0	HOI	thermodynamically impossible
-1	1	I_2OH^-	-
-1	2	I_3OH^{-2}	curved
0	-1	H_2O_2 or O	thermodynamically impossible
0	1	$I_2O^{=}$	straight line
0	2	I_3O^{-3}	curved
1	-1	HO_2^-	thermodynamically impossible
1	0	IO_2H^{-2}	curved with a maximum
1	1	$I_2O_2H^{-3}$	possibly a straight line
1	2	$I_3O_2H^{-4}$	curved
2	-1	O_2^{-2}	thermodynamically impossible
2	0	IO_2^{-3}	curved
2	1	$I_2O_2^{-4}$	curved with a maximum
2	2	$I_3O_2^{-5}$	curved

* $IO^- + xOH^- + yI^- \rightleftharpoons$ the fourth species

with corrections for ionic strength will be given later. As shown in Table IX, when x = 0 and y = 1, the fourth species is $I_2O^{=}$. In other words, the equilibrium is as follows:

$$IO^- + I^- \underset{\longleftarrow}{\overset{K_4}{\longrightarrow}} I_2O^{=} \quad . \tag{19}$$

As indicated in Table IX, neither with y = 0 nor y = 2 could a straight line be drawn; this result agreed with the previous consideration that neither IO^- nor I_3^- could be the species tied up by OH^-.

(B) Calculation of the Equilibrium Constants from the Spectrophotometric Results

With the presence of $I_2O^{=}$ established, it is of interest to go back to Eq. (11) and recalculate the equilibrium constants (i.e. K_1, K_2, and Q_4). In view of Eqs. (4) and (8), it was considered that the dependence of the values of K_1 and K_2 on the ionic strength would be small because equal numbers of monovalent ions were present on both sides of the chemical equations. Therefore activity-coefficient corrections were ignored for K_1 and K_2. The same is not true in the case of K_4 (Eq. (19)) which is most likely to be greatly affected by the ionic strength. In Eq. (20), if a represents activity and γ represents the activity coefficient, we have

$$K_4 = \frac{a_{I_2O^{=}}}{a_{IO^-}\, a_{I^-}} = \frac{\gamma_{I_2O^{=}}\,(I_2O^{=})}{\gamma_{I^-}\,\gamma_{IO^-}(IO^-)(I^-)} = \frac{Q_4\,\gamma_{I_2O^{=}}}{\gamma_{I^-}\,\gamma_{IO^-}} \quad . \tag{20}$$

Thus K_4 is the value of Q_4 at zero ionic strength. In order to estimate the value of $\gamma_{I_2O^{=}}$ and γ_{IO^-}, a method of analogy has to be used. Suppose the activity coefficient of Na_2SO_4 [18] is used to substitute for Na_2I_2O

and that of $NaClO_4$ [18] is used for NaIO as well as NaI. Then we have

$$K_4 = Q_{4,\mu}\left(\frac{\gamma_{I_2O^=}}{\gamma_{I^-}\,\gamma_{IO^-}} \right)_\mu = Q_{4,\mu} \Big/ \left[\frac{\gamma_{I^-}\,\gamma_{IO^-}}{\gamma_{I_2O^=}} \times \frac{\gamma_{Na^+}\,\gamma_{Na^+}}{\gamma_{Na^+}\,\gamma_{Na^+}} \right]_\mu$$

$$= Q_{4,\mu} \Big/ \left[\frac{\gamma^2_{\pm NaI}\,\gamma^2_{\pm NaIO}}{\gamma^3_{\pm Na_2I_2O}} \right]_\mu \cong Q_{4,\mu} \Big/ \left(\frac{\gamma^4_{\pm NaClO_4}}{\gamma^3_{\pm Na_2SO_4}} \right)_\mu = Q_{4,\mu} / \gamma_\mu \quad , \quad (21)$$

where μ represents the ionic strength of the experiment and

$$\gamma_\mu = \left(\gamma^4_{\pm NaClO_4} / \gamma^3_{\pm Na_2SO_4} \right)_\mu .$$

The value of γ_μ changes from 2 to about 4.5 as the ionic strength increases from 0.15 to 1.5. With the knowledge of the presence of $I_2O^=$ and the correction for ionic strength, one can rewrite Eq. (18) as follows:

$$\frac{(\bar{\epsilon}_1 - \bar{\epsilon}_2)\left[1 + K_1 \frac{(I^-)}{(OH^-)} + K_2 \frac{(I^-)^2}{(OH^-)^2} + K_4\,\gamma_1(I^-)_1\right]}{\left[1 + \frac{K_1(I^-)}{(OH^-)} + \frac{K_2(I^-)^2}{(OH^-)^2}\right]} \times$$

$$\frac{\left[1 + K_1 \frac{(I^-)}{(OH^-)} + K_2 \frac{(I^-)^2}{(OH^-)^2} + K_4\gamma_2(I^-)_2\right]}{\left[\gamma_1(I^-)_1 - \gamma_2(I^-)_2\right]} + \frac{\frac{K_2(I^-)^2}{(OH^-)^2}\left(\epsilon_{I_3^-} - \epsilon_{I_3^-}\right)}{\left[\gamma_1(I^-)_1 - \gamma_2(I^-)_2\right]}$$

$$= K_4\epsilon_{I_2O^=} - K_4\left\{ \frac{\left[\epsilon_{IO^-} + \epsilon_{I_2OH^-}\frac{K_1(I^-)}{(OH^-)}\right] - \frac{\frac{K_2(I^-)^2}{(OH^-)^2}\left[\epsilon_{I_3^-}\gamma_2(I^-)_2 - \epsilon_{I_3^-}\gamma_1(I^-)_1\right]}{\gamma_1(I^-)_1 - \gamma_2(I^-)_2}}{1 + \frac{K_1(I^-)}{(OH^-)} + \frac{K_2(I^-)^2}{(OH^-)^2}} \right\} . \quad (22)$$

As mentioned earlier in this report, $\epsilon_{I_3^-}$ was found to vary linearly with respect to (I^-) in the wavelength range of our study according to

$$\epsilon_{I_3^-} = \epsilon_{I_{3_0}^-} + \alpha(I^-) \ , \tag{23}$$

where $\epsilon_{I_{3_0}^-}$ is the molar absorptivity of I_3^- at zero iodide concentration and α is a constant. From Eq. (23), one obtains

$$\frac{[\epsilon_{I_{3_1}^-}\gamma_2(I^-)_2 - \epsilon_{I_{3_2}^-}\gamma_1(I^-)_1]}{\gamma_1(I^-)_1 - \gamma_2(I^-)_2} =$$

$$\frac{[\epsilon_{I_{3_0}^-} + \alpha(I^-)_1]\gamma_2(I^-)_2 - [\epsilon_{I_{3_0}^-} + \alpha(I^-)_2]\gamma_1(I^-)_1}{\gamma_1(I^-)_1 - \gamma_2(I^-)_2} = \frac{-\epsilon_{I_{3_0}^-}[\gamma_1(I^-)_1 - \gamma_2(I^-)_2]}{\gamma_1(I^-)_1 - \gamma_2(I^-)_2}$$

$$+ \frac{\alpha(I^-)_1(I^-)_2(\gamma_2 - \gamma_1)}{\gamma_1(I^-)_1 - \gamma_2(I^-)_2} = -\epsilon_{I_{3_0}^-} + \frac{\alpha(I^-)_1(I^-)_2(\gamma_2 - \gamma_1)}{\gamma_1(I^-)_1 - \gamma_2(I^-)_2} \ . \tag{24}$$

Substituting Eq. (24) into Eq. (22), one can rewrite the latter as

$$\frac{(\bar{\epsilon}_1 - \bar{\epsilon}_2)[1 + \frac{K_1(I^-)}{(OH^-)} + \frac{K_2(I^-)^2}{(OH^-)^2} + K_4\gamma_1(I^-)_1][1 + \frac{K_1(I^-)}{(OH^-)} + \frac{K_2(I^-)^2}{(OH^-)^2} + K_4\gamma_2(I^-)_2]}{[1 + \frac{K_1(I^-)}{(OH^-)} + \frac{K_2(I^-)^2}{(OH^-)^2}]\,[\gamma_1(I^-)_1 - \gamma_2(I^-)_2]}$$

$$+ \frac{\frac{K_2(I^-)^2}{(OH^-)^2}\,(\epsilon_{I_3^-{}_2} - \epsilon_{I_3^-{}_1})}{[\gamma_1(I^-)_1 - \gamma_2(I^-)_2]} = K_4\epsilon_{I_2O} =$$

$$-K_4\left\{ \frac{[\epsilon_{IO^-} + \epsilon_{I_2OH^-}\frac{K_1(I^-)}{(OH^-)} + \epsilon_{I_3^-{}_0}\frac{K_2(I^-)^2}{(OH^-)^2}]}{1 + K_1\frac{(I^-)}{(OH^-)} + K_2\frac{(I^-)^2}{(OH^-)^2}} - \frac{K_2\frac{(I^-)^2}{(OH^-)^2}\frac{\alpha(I^-)_1(I^-)_2(\gamma_2 - \gamma_1)}{\gamma_1(I^-)_1 - \gamma_2(I^-)_2}}{1 + K_1\frac{(I^-)}{(OH^-)} + K_2\frac{(I^-)^2}{(OH^-)^2}} \right\},$$

Let

$$\frac{\frac{K_2(I^-)^2}{(OH^-)^2}\,\frac{\alpha(I^-)_1(I^-)_2(\gamma_2 - \gamma_1)}{\gamma_1(I^-)_1 - \gamma_2(I^-)_2}}{1 + K_1\frac{(I^-)}{(OH^-)} + K_2\frac{(I^-)^2}{(OH^-)^2}} = S.$$

Then we have

$$\frac{(\bar{\epsilon}_1 - \bar{\epsilon}_2)[1 + \frac{K_1(I^-)}{(OH^-)} + \frac{K_2(I^-)^2}{(OH^-)^2} + K_4\gamma_1(I^-)_1][1 + \frac{K_1(I^-)}{(OH^-)} + \frac{K_2(I^-)^2}{(OH^-)^2} + K_4\gamma_2(I^-)_2]}{[1 + \frac{K_1(I^-)}{(OH^-)} + \frac{K_2(I^-)^2}{(OH^-)^2}][\gamma_1(I^-)_1 - \gamma_2(I^-)_2]}$$

$$+ \frac{\frac{K_2(I^-)^2}{(OH^-)^2}(\epsilon_{I_{3_2}^-} - \epsilon_{I_{3_1}^-})}{[\gamma_1(I^-)_1 - \gamma_2(I^-)_2]} = K_4 \left\{ \epsilon_{I_2O^=} - [\bar{\epsilon}_{00} - S] \right\} \qquad (25)$$

where $\bar{\epsilon}_{00}$ corresponds to the effective molar absorptivity at zero iodide and zero hydroxide concentrations but at a relevant ratio of (I^-) to (OH^-). The term "S" was always found to be negligibly small compared with $\bar{\epsilon}_{00}$. When the quantity on the left side (R) of Eq. (25) was computed with the experimental results of Table VIII at 289.9 mμ and was plotted against the values of $(\bar{\epsilon}_{00} - S)$, a straight line was obtained. The values of K_1 and K_2 used here for the first approximation were those from the previous calculation in this report (i.e. $K_1 = 0.12$ and $K_2 = 4.5 \times 10^{-3}$). The slope of the line is K_4, and the intercept is $K_4\epsilon_{I_2O^=}$. By the use of the same method of successive approximations as used before, a value for K_4 of 0.045 was obtained from the straight line of Fig. 12. This value is much smaller than that of Q_4 from the previous calculation in this report because of the activity-coefficient correction. This result of K_4 was confirmed when the data at 320.1 mμ were treated in the same way as at 289.9 mμ. For the other two wavelengths (i.e. 400.6 mμ and 360.5 mμ), where the effect of $I_2O^=$ is smaller, 0.045 was

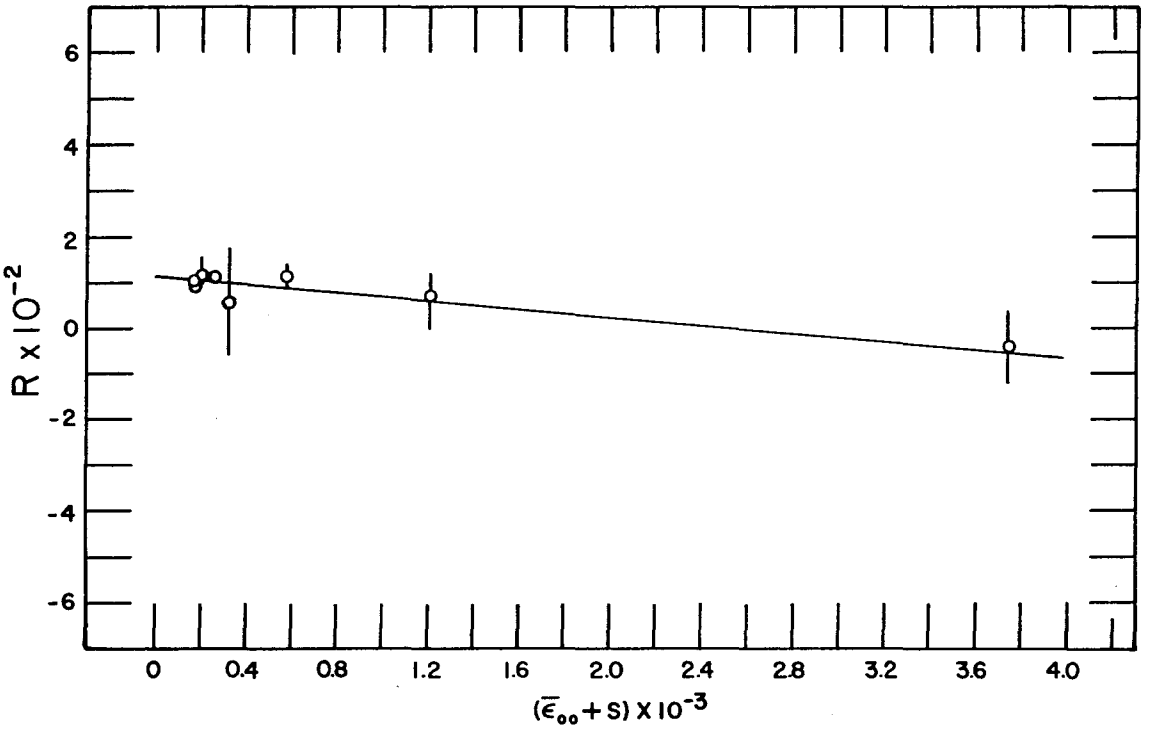

Fig. 12. Plot of R vs $(\bar{\epsilon}_{00} + S)$. $\lambda = 289.9$ mμ.

assumed as the slope of the line and was combined with the data of three pairs of experiments of Table VIII (i.e. the three pairs containing Experiments II-X-1, IV-M-1, and IV-R-2) to calculate the average values of $\epsilon_{I_2O^=}^{400.6}$ and $\epsilon_{I_2O^=}^{360.5}$. The uncertainties of the points shown in Fig. 12 were calculated from the probable error of $(\bar{\epsilon}_1 - \bar{\epsilon}_2)$. The upper and lower limits of the values of $\bar{\epsilon}_1$ and $\bar{\epsilon}_2$ were first estimated at 400.6 mμ on the basis of the uncertainty in extrapolating the A-t curves to zero time. The same percentage uncertainty was used at the other wavelengths. Because the value of Q_4 was greatly influenced by ionic strength and estimated activity-coefficients had to be used for the calculation, the value of K_4 is not considered to be an accurate one. The correction for ionic strength did show apparent improvement in giving a straight-line fit to the experimental points (Fig. 12). From the magnitude of K_4 obtained in this investigation, one sees that under experimental conditions where the initial hydroxide concentration is equal to or lower than 0.100 M and the ionic strength is also small, the ratio between the concentrations of I_2OH^- and $I_2O^=$ is quite large, i.e. the correction for $I_2O^=$ is small.

Although the contribution of $I_2O^=$ to the effective molar absorptivity of experiments with hydroxide concentration equal to or lower than 0.100 M was small, it was desirable to correct the latter to zero hydroxide and zero iodide concentrations (at a constant ratio of (I^-) to (OH^-), so as to get more precise values of K_1 and K_2. By assuming that in Eq. (25), Experiment 1 is the one to be corrected and Experiment 2 is the one with zero iodide and zero hydroxide concentrations (i.e. $\bar{\epsilon}_2 = \bar{\epsilon}_{00}$), one can rearrange Eq. (25) as follows:

$$\bar{\epsilon}_1 - \bar{\epsilon}_{00} = \frac{(\epsilon_{I_2 0} - \bar{\epsilon}_1) + \dfrac{\dfrac{K_2(I^-)^2}{(OH^-)^2}}{K_4\gamma_1(I^-)_1}(\epsilon_{I_3^-{}_1} - \epsilon_{I_3^-{}_0})}{\dfrac{[1 + \dfrac{K_1(I^-)}{(OH^-)} + \dfrac{K_2(I^-)^2}{(OH^-)^2} + K_4\gamma_1(I^-)_1]}{K_4\gamma_1(I^-)_1} - 1} \quad . \quad (26)$$

This correction of $\bar{\epsilon}$ according to Eq. (26) is based upon the assumption that the changing of the molar absorptivity of I_3^- as a linear function of the iodide concentration is due to a solvent effect on the molar absorptivity, i.e. Eq. (23) was used in the correction. Alternatively one could attribute the change in molar absorptivity to the presence of a new species which is in equilibrium with I_3^- and contributes a different light absorption. It was found that this latter method of correction did not give the same value of $\bar{\epsilon}_{00}$ as that of the previous method because there was no information on the magnitude of either the molar absorptivity of that unknown species or the equilibrium constant between it and triiodide, an exact correction of $\bar{\epsilon}$ could not be made with this alternative method. It is believed that the difference of the two corrections probably is not large, although it might be appreciable. Davies and Gwynne[19] studied the equilibrium between I_2, I^-, and I_3^- by solvent partition at 25°C in a range of iodide concentration from 0.02 M to 1 M. No evidence of the presence of a new species was reported. Although their assumption of cancellation of the activity coefficients of I_3^- and I^- may not be strictly valid, yet it is considered that their results give good reason for using the solvent-effect model to correct the $\bar{\epsilon}$ in this investigation.

All values of $\bar{\epsilon}$ of Table VIII at the four wavelengths were corrected to $\bar{\epsilon}_{00}$ by the use of Eq. (26). The $\bar{\epsilon}_{00}$ values of the experiments with $(OH^-) \leq 0.100$ M were used in Eq. (12) to calculate Y by letting $\bar{\epsilon} = \bar{\epsilon}_{00}$. When different values of K_1 were tried and the plots of Y_{00} versus $(\bar{\epsilon}_{I_3^-} - \bar{\epsilon}_{00})(I^-)/(OH^-)$ were made for 400.6 mμ, 360.5 mμ, and 320.1 mμ as well as 289.9 mμ, the best value of K_1, i.e. that which made the experimental points at the four wavelengths fall upon the master curve best, was found to be 0.13. The data from which the plots were made are tabulated in Tables X and XI. The upper and lower limits of the value of $\bar{\epsilon}_{00}$ were obtained by the use of the corresponding limits of $\bar{\epsilon}_1$ in Eq. (26). The method of estimation of the uncertainty of $\bar{\epsilon}_1$ was the same as reported earlier. The data along with the superimposed master curve are shown in Figs. 13 to 16. The values of the equilibrium constants from the spectrophotometric results are as follows:

$$IO^- + I^- + H_2O \underset{}{\overset{K_1}{\rightleftharpoons}} I_2OH^- + OH^- \qquad \left[K_1 = \frac{(I_2OH^-)(OH^-)}{(IO^-)(I^-)} = 0.13\right];$$

$$IO^- + 2I^- + H_2O \underset{}{\overset{K_2}{\rightleftharpoons}} I_3^- + 2OH^- \qquad \left[K_2 = \frac{(I_3^-)(OH^-)^2}{(IO^-)(I^-)^2} = 5.1 \times 10^{-3}\right];$$

$$IO^- + I^- \underset{}{\overset{K_4}{\rightleftharpoons}} I_2O^= \qquad [K_4 = a_{I_2O^=} / a_{IO^-}\, a_{I^-} = 0.045].$$

The molar absorptivities of I_2OH^- and $I_2O^=$ are given in Table XII. The values of $\epsilon_{I_2OH^-}$ were calculated from the results of Experiment II-H-5 of Table VIII by the use of the known equilibrium constant and on the assumption that the effect due to $I_2O^=$ was negligible at the hydroxide concentration used, i.e. 0.100 M. These calculated results at 400.6 mμ, 360.5 mμ, 320.1 mμ, and 289.9 mμ were compared with those read from the

plots of Figs 13 to 16. They were found to be in agreement to within 5% except at 360.5 mμ, where the deviation was about 13%. The reported values of $\epsilon_{I_2OH^-}$ and $\epsilon_{I_2O^=}$ in Table XII at the four wavelengths mentioned above were those from the plots. The absorption spectrum of I_2OH^-, which was present in equilibrium with $I_2O^=$ in Experiment II-H-5, is shown in Fig. 17. The uncertainties shown were estimated by allowing $\pm$ 0.005 error in the absorbance. The values contain any additional error arising from errors in K_1 and K_2 and neglect of $I_2O^=$.

(C) Discussion

The species I_2OH^- is believed to be analogous to I_3^- with OH^- substituted for the I^-. As to $I_2O^=$, presumably it is an ionization product of I_2OH^-. The electronic arrangement of I_3^- has been discussed by Pauling,[20] Kimball,[21] and Pimentel.[22] The latter explained the bonding in trihalide ions by presenting a simple molecular orbital treatment and suggested the possibility of predicting the stability of other molecular species having electronic structures like those of the trihalide ions. According to this kind of prediction, the hydroxide ion, which is isoelectronic with I^-, should be able to combine with the I_2 molecule to form I_2OH^-.

Near the close of this investigation, it was found that Kennedy[23] had suggested I_2OH^- as an intermediate in the hydrolysis of iodine in order to fit the rate law found for the reaction of n-propanol with iodine in ca. 1 M $HClO_4$. Alternative explanations are possible. Recently Anbar and Taube[12] have proposed Cl_2OH^- as a possible intermediate in the exchange reaction between Cl^- and HOCl. They suggested that the structure

Table X

The effective molar absorptivities

at zero iodide and zero hydroxide concentrations*

Exp't. No.	$(I^-)/(OH^-)$	$\bar{\epsilon}_{00}^{400.6}$	$Y_{00}^{400.6}$	$X_{00}^{400.6}$ ($\times 10^{-3}$)	$\bar{\epsilon}_{00}^{360.5}$	$Y_{00}^{360.5}$	$X_{00}^{360.5}$ ($\times 10^{-3}$)
		41.5	30.6	0.595	66.2	90.9	2.45
II-X-1	0.1000	40.5	20.4	0.595	65.2	80.8	2.45
		39.5	10.3	0.595	64.2	70.6	2.45
		40.4	19.4	0.595	65.4	82.8	2.45
IV-M-1	0.1000	39.4	9.27	0.595	64.4	72.6	2.45
		38.4	-	-	63.4	62.5	2.45
		55.9	41.4	2.97	121.6	143.6	12.21
II-G-1	0.5000	52.6	34.2	2.97	114.4	128.2	12.22
		50.4	29.6	2.97	103.9	105.8	12.22
		76.5	47.8	5.91	211	181.3	24.3
II-H-5	1.000	72.6	43.3	5.92	201	169.9	24.3
		69.4	39.7	5.92	191.6	159.3	24.4
		169.6	88.0	11.64	535	310	48.0
II-H-7	2.000	139.3	68.9	11.70	423	239	48.3
		118.0	55.3	11.74	349	192.2	48.4
		487	154.8	27.5	1927	632	113.1
II-J-1	5.000	472	149.8	27.6	1870	613	113.4
		456	144.6	27.7	1811	594	113.7
		508	161.0	27.6	1967	642	114.0
**II-K-1	5.027	497	157.3	27.7	1930	630	114.0
		476	150.5	27.8	1852	604	114.5
		1222	282	47.7	4.92×10^3	1145	196.3
II-U-1	10.00	1142	264	48.5	4.63×10^3	1077	199.2
		1115	257	48.8	4.53×10^3	1053	200
		2.18×10^3	398	76.3	8.88×10^3	1631	314
II-L-2	20.00	2.13×10^3	390	77.2	8.72×10^3	1603	317

*$K_1 = 0.134$; $\lambda = 400.6$ mμ and 360.5 mμ;

$X_{00} = (\epsilon_{I_3^-}^{\circ} - \bar{\epsilon}_{00})[(I^-)/(OH^-)]$; and $Y_{00} = [\bar{\epsilon}_{00} - \epsilon_{IO^-}^{\circ} + \bar{\epsilon}_{00} K_1(I^-)/(OH^-)] \div [(I^-)/(OH^-)]$.

** I_3^- was used as the starting material.

Table XI

The effective molar absorptivities

at zero iodide and zero hydroxide concentrations*

Exp't. No.	$(I^-)/(OH^-)$	$\epsilon_{00}^{320.1}$	$Y_{00}^{320.1}$	$X_{00}^{320.1}$ ($\times 10^{-3}$)	$\epsilon_{00}^{289.9}$	$Y_{00}^{289.9}$ ($\times 10^{-3}$)	$X_{00}^{289.9}$ ($\times 10^{-3}$)
		56.8	95.6	1.394	169.8	0.378	3.98
II-X-1	0.1000	55.8	85.5	1.394	167.8	0.357	3.98
		54.8	75.4	1.395	165.8	0.337	3.98
		56.1	88.3	1.394	164.6	0.325	3.98
IV-M-1	0.1000	55.2	79.4	1.395	162.6	0.305	3.98
		54.1	68.3	1.395	160.6	0.285	3.98
		105.8	129.8	6.95	332	0.440	19.83
II-G-1	0.5000	99.5	116.4	6.95	313	0.399	19.84
		95.1	107.0	6.95	299	0.369	19.85
		168.8	143.4	13.83	555	0.495	39.4
II-H-5	1.000	160.2	133.7	13.84	524	0.460	39.5
		152.9	125.4	13.85	501	0.434	39.5
		411	237	27.2	1348	0.787	77.3
II-H-7	2.000	335	188.5	27.3	1100	0.630	77.8
		285	156.7	27.4	942	0.530	78.1
		1252	409	63.7	3.80×10^3	1.244	181.0
II-J-1	5.000	1212	395	63.9	3.70×10^3	1.209	181.5
		1174	382	64.1	3.58×10^3	1.170	182.1
		1304	427	64.0	3.96×10^3	1.288	181.9
**II-K-1	5.027	1278	418	64.2	3.87×10^3	1.260	182.0
		1230	402	64.4	3.73×10^3	1.215	183.0
		3.09×10^3	718	109.1	9.23×10^3	2.15	308
II-U-1	10.00	2.91×10^3	677	110.9	8.85×10^3	2.06	312
		2.85×10^3	662	111.5	8.67×10^3	2.02	313
		5.51×10^3	1013	169.9	1.616×10^4	2.97	477
II-L-2	20.00	5.41×10^3	994	171.8	1.593×10^4	2.92	481

$K_1 = 0.134$; $\lambda = 320.1$ mμ and 289.9 mμ ;

$X_{00} = (\epsilon_{I_3^-}{}_0 - \bar{\epsilon}_{00})[(I^-)/(OH^-)]$; and $Y_{00} = [\bar{\epsilon}_{00} - \epsilon_{IO^-} + \bar{\epsilon}_{00}K_1(I^-)/(OH^-)] \div [(I^-)/(OH^-)]$.

**I_3^- was used as the starting material.

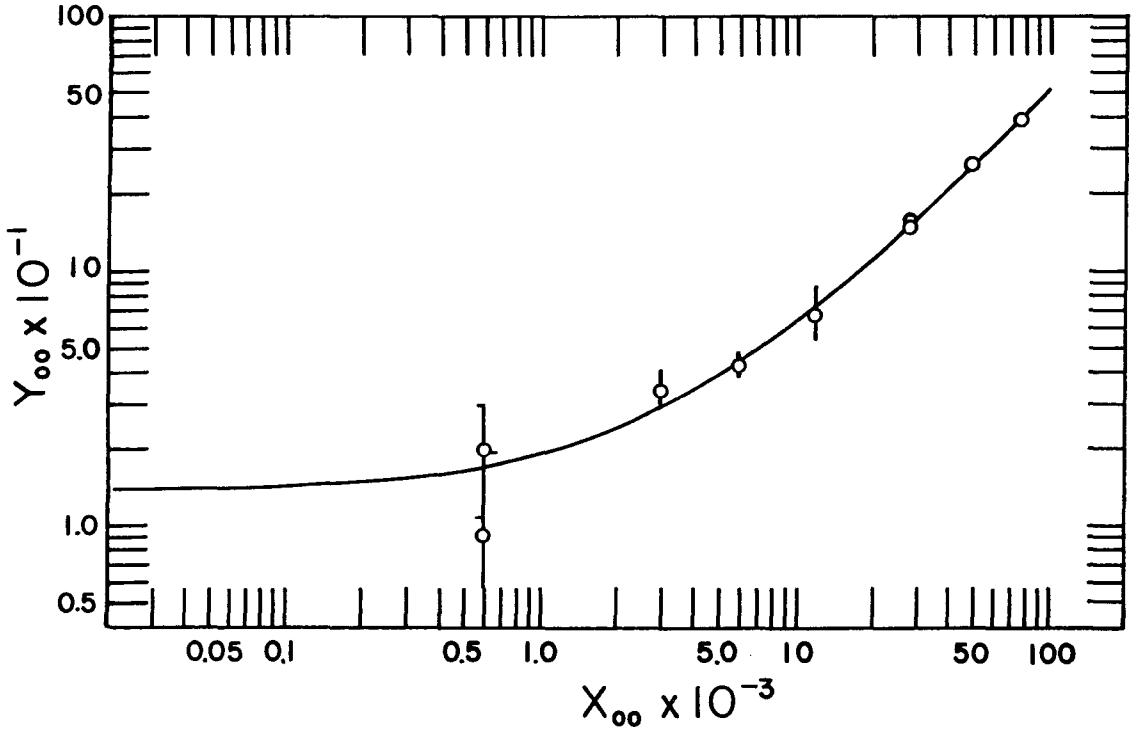

Fig. 13. Plot of Y_{00} vs X_{00} of Table X. λ = 400.6 mμ.

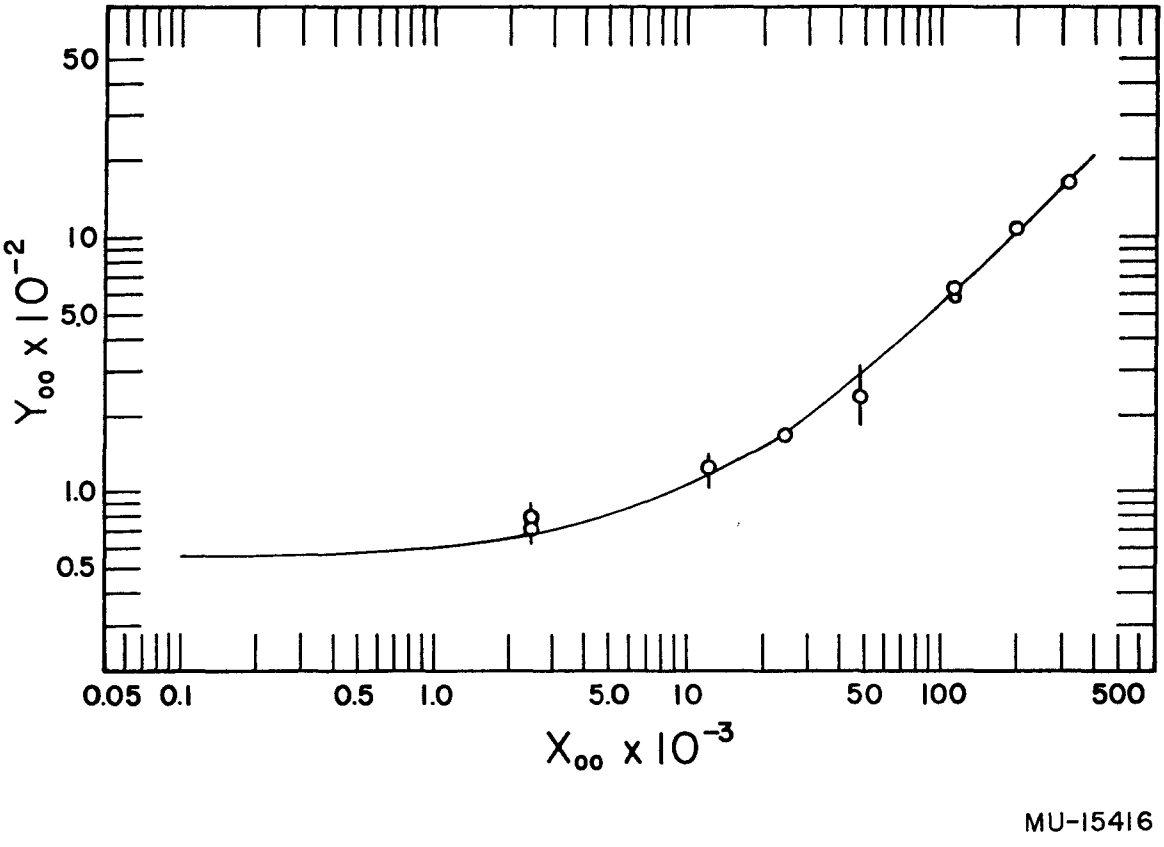

Fig. 14. Plot of Y_{00} vs X_{00} of Table X. λ = 360.5 mμ.

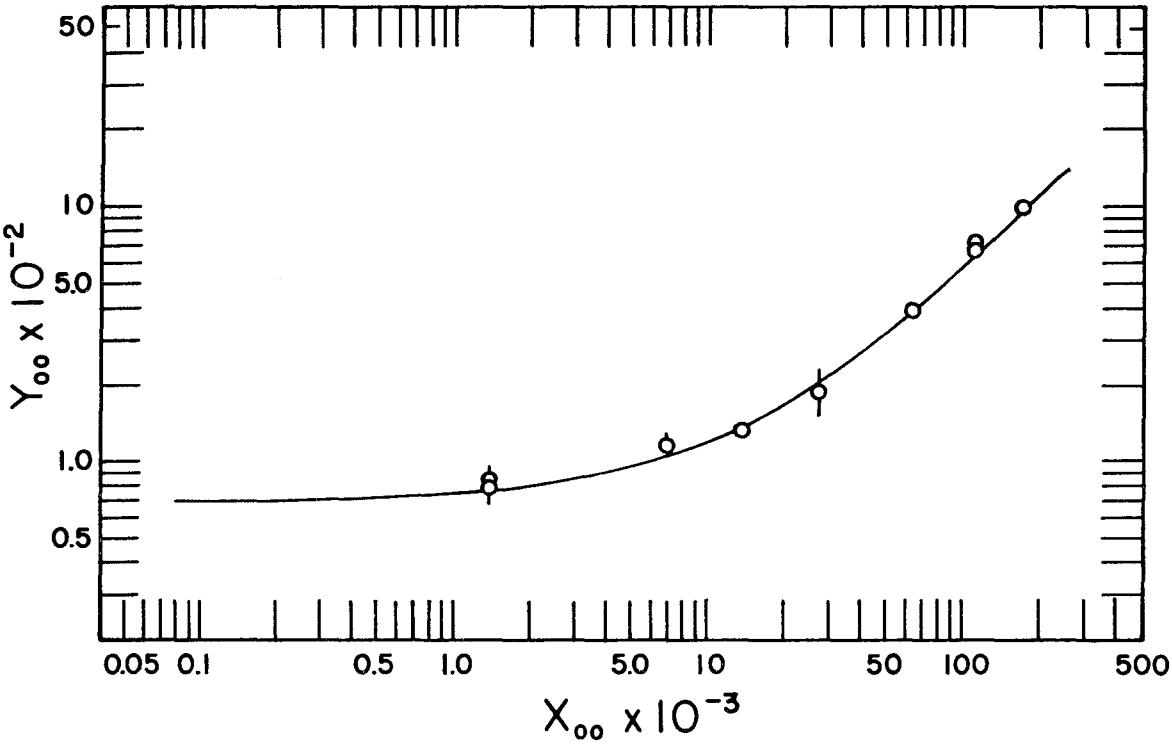

Fig. 15. Plot of Y_{00} vs X_{00} of Table XI. λ = 320.1 mμ.

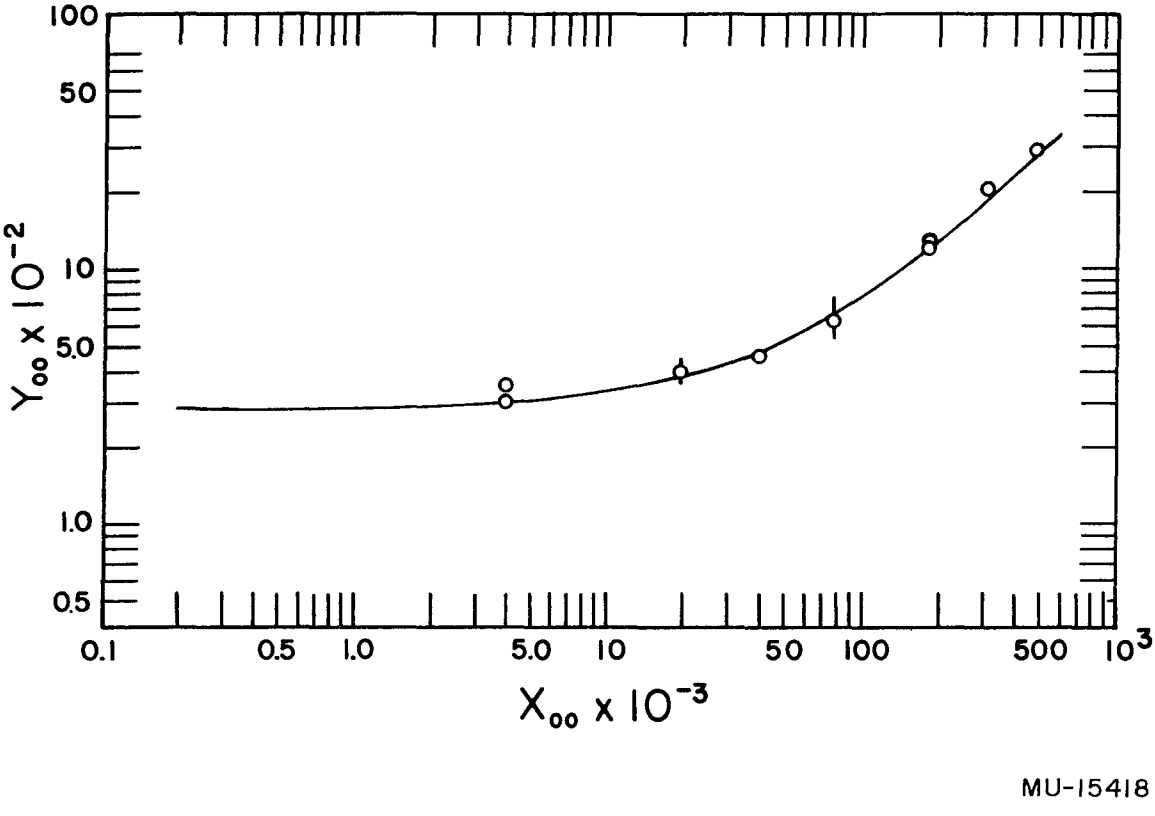

Fig. 16. Plot of Y_{00} vs X_{00} of Table XI. λ = 289.9 mμ.

Table XII

The molar absorptivities of I_2OH^- and $I_2O^=$

λ (mμ)	$\epsilon_{I_2OH^-} \times 10^{-2}$	$\epsilon_{I_2O^=} \times 10^{-2}$
400.6	1.0	0.60
393.0	1.3	-
382.2	1.9	-
371.6	2.7	-
360.5	4.2	3.3
350.8	4.6	-
340.5	4.7	-
330.2	4.7	-
320.1	5.2	3.5
310.0	6.6	-
299.9	11	-
289.9	22	26
280.0	43	-

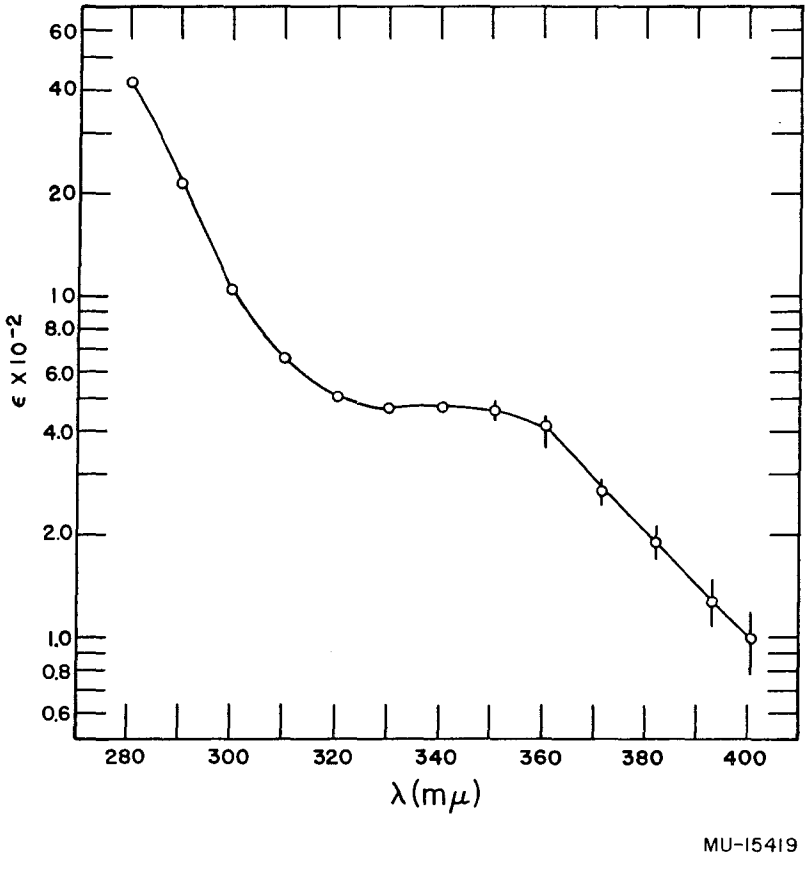

Fig. 17. The absorption spectrum of I_2OH^- from Experiment II-H-5 of Table VIII.

of Cl_2OH^- is analogous to that of Br_3^-, which is the same analogy as that used in this investigation between I_3^- and I_2OH^-.

By knowing the values of K_1 and K_4, one can calculate the ionization constant of I_2OH^-,

$$I_2OH^- \overset{K_{I_2OH^-}}{\rightleftharpoons} I_2O^= + H^+ , \qquad (27)$$

where $K_{I_2OH^-} = (I_2O^=)(H^+)/(I_2OH^-) = K_4K_{H_2O}/K_1 = 3.3 \times 10^{-15}$. Comparing this value with the result of the ionization constant of HOI (2.3×10^{-11}), which will be reported later, one finds that there is a factor of 7000 between the two ionization constants, with I_2OH^- being a much weaker acid than HOI. One would probably predict this because there is a negative charge on I_2OH^- as well as one pair of electrons above that for an octet structure, both of which factors would make the proton harder to remove than from HOI.

(D) EMF Measurements

Attempts were made to determine the potential of the I^- - IO^- couple in 1 M OH^- solution by measuring the emf of the cell

$$Pt : H_2 : 1\ M\ NaOH : 1\ M\ NaOH, KI, NaIO : Au\ (or\ Pt), \qquad (28a)$$

or, in other words, to measure the potential of the following reaction

$$H_2 + IO^- = H_2O + I^- . \qquad (28b)$$

It was hoped that a more precise value of K_2 (Eq. (4)) could be obtained, and, by use of it with the spectrophotometric results, one could then improve the accuracy of the value of K_1.

(1) Experimental Procedure

A sodium hydroxide solution of the desired concentration was put into

cell C and the four bubblers (Q_1, Q_2, R_1, and R_2), as described earlier. Cell A and the hydrogen electrodes which had been platinized were also placed in position. The cell was then put into the 25.00 $\pm$ 0.01°C water bath and left there in order to establish temperature equilibrium as well as to attain equilibrium at the hydrogen electrodes. Hydrogen gas from two separate tanks was gently passed first through alkaline pyrogallol solutions in 250-ml gas-washing bottles, then to the inlet bubblers, and finally through the tubes M and N to the hydrogen electrodes. The two hydrogen electrodes were measured against one another. It was assumed that equilibrium conditions were attained when the emf reading of the two electrodes was found to be 0.02 mv or less. This could be reached within an hour or two if the solution in cell C had been presaturated with the same hydrogen gas and the electrodes had been properly platinized. The central part of cell C where cell A was placed was covered with aluminum foil to exclude any light effect.

The process of mixing basic iodide and hypochlorite was carried out with the same procedure as used in the spectrophotometric study. The reaction mixture was quickly transferred to cell A through a long-stem funnel which was inserted into the cell through the third opening (G_3). The emf readings of the cell were taken immediately after the sample was introduced into A with gold and platinum electrodes successively. The measurement was carried out as a function of time. Frequently the electrode was lifted from the cell, and the solution in A was stirred by using the electrode as a stirrer. The emf readings were taken before and after stirring to see whether there was any stirring effect. The balance of the hydrogen electrodes was checked from time to time during an experiment.

(2) Measurement of $IO^- - I_3^- - I^-$ Equilibrium

As indicated above, both gold and platinum electrodes were used in the measurement of emf of Eq. (28a). Only the results using a gold electrode in the IO^- compartment will be reported here however, because the platinum electrode was found to be greatly affected by stirring. This effect will be discussed later. Attempts were made to correct for the liquid-junction potential by using Henderson's equation.[24] The result was found to be negligibly small. The data used in calculating the value of K_2 of the equilibrium between IO^-, I_3^-, and I^- (Eq. (4)) are presented in Table XIII. The concentrations listed in columns 2 to 4 were all in moles per liter. The fifth column records the observed emf reading at zero time, which was obtained by extrapolating to zero time the curve of emf versus time (emf-t). A typical emf-t curve is indicated in Fig. 18. (Experiment V-C-1). The solid circles indicate measurement after stirring. The sixth column of Table XIII represents the standard potential of Eq. (28b) and was obtained from the following equation:

$$E^\circ(\text{total}) = E_0(\text{cell}) + \left(\frac{0.05916}{2}\right) \log\left[\frac{(I^-)_{in} - (IO^-)_{in}}{(IO^-)_{in}}\right], \quad (29)$$

where $(I^-)_{in}$ and $(IO^-)_{in}$ were respectively the initial concentrations of I^- and IO^- in the experiment, and the activity-coefficient correction to zero ionic strength has been assumed negligible. By knowing $E^\circ(\text{total})$ and $E_B^\circ(H_2 - H_2O)$ of Eq. (30), one can then calculate the value of E_B° $(I^- - IO^-)$ (Eq. (31)) from

$$H_2 + 2OH^- = 2H_2O + 2e^- \qquad [E_B^\circ(H_2\text{-}H_2O) = 0.82824 \text{ volt}^{18}], \quad (30)$$

$$2OH^- + I^- = IO^- + H_2O + 2e^- \; [E_B^\circ(I^- - IO^-)]. \quad (31)$$

Table XIII

EMF measurement of $IO^- - I_3^- - I^-$ equilibrium*

Exp't. No.	$(I^-)_{in}$ ($\times 10^3$ M)	$(ClO^-)_{in}$ ($\times 10^3$ M)	$(Cl^-)_{in}$ ($\times 10^3$ M)	E_0(cell) (volts)	E^o(total) (volts)	$E_B^o(I^- - IO^-)$ (volt)	$E_B^o(IO^- - I_3^-)$ (volt)	K_2 ($\times 10^3$)
V-A-2	102.0	2.000	-	1.24680	1.29706	-0.46882	-0.0667	5.56
V-B-2	105.0	5.000	-	1.25895	1.29743	-0.46919	-0.0663	5.74
V-C-1	35.33	2.000	66.67	1.26105	1.29719	-0.46895	-0.0665	5.65

*$(OH^-)_{in}$ = 1.000 M

Subtracting Eq. (31) from Eq. (30), one has

$$H_2 + IO^- = H_2O + I^- \qquad [\ E^o(\text{total})\ ]\ . \qquad (28b)$$

Therefore, one obtains

$$E_B^o\ (I^- - IO^-) = E_B^o\ (H_2 - H_2O) - E^o(\text{total}). \qquad (32)$$

The results for $E_B^o\ (I^- - IO^-)$ are reported in column 7. The $E_B^o\ (IO^- - I_3^-)$ values in column 8 were defined as the standard potential of Eq. (4), which could easily be obtained by subtracting Eq. (31) from Eq. (33):

$$3I^- = I_3^- + 2e^- \qquad [\ E^o = -0.5355 \text{ volt } ^{18}]. \qquad (33)$$

Subtracting, one finds

$$IO^- + 2I^- + H_2O \underset{\longleftarrow}{\xrightarrow{K_2}} I_3^- + 2OH^- \quad [E_B^o(IO^- - I_3^-)]. \qquad (4)$$

Finally by the use of the relation $E_B^o(IO^- - I_3^-) = (0.05916/2) \log K_2$, one obtains the values of K_2 in column 9.

(3) Calculation of the Ionization Constant of HOI

From the results for K_2 listed in Table XIII, and the known equilibrium constants of Eqs. (2), (6) and (7), one can calculate the ionization constant of hypoiodous acid in the following way. We have

$$IO^- + 2I^- + H_2O \underset{\longleftarrow}{\xrightarrow{K_2}} I_3^- + 2OH^- \quad [K_2 = (I_3^-)\ (OH^-)^2/(IO^-)(I^-)^2 = 5.65 \times 10^{-3}], \ (4)$$

$$H_2O \underset{\longleftarrow}{\xrightarrow{K_{H_2O}}} H^+ + OH^- \qquad [K_{H_2O} = (H^+)(OH^-) = 10^{-14}], \ (2)$$

$$I_2 + I^- \underset{\longleftarrow}{\xrightarrow{K_6}} I_3^- \qquad [K_6 = (I_3^-)/(I^-)(I_2) = 7.14 \times 10^2], (6)^{18}$$

and

$$I_2 + H_2O \underset{\longleftarrow}{\xrightarrow{K_7}} HOI + I^- + H^+ \qquad [K_7 = (HOI)(H^+)(I^-)/(I_2) = 5.40 \times 10^{-13}]\ . \qquad (7)^2$$

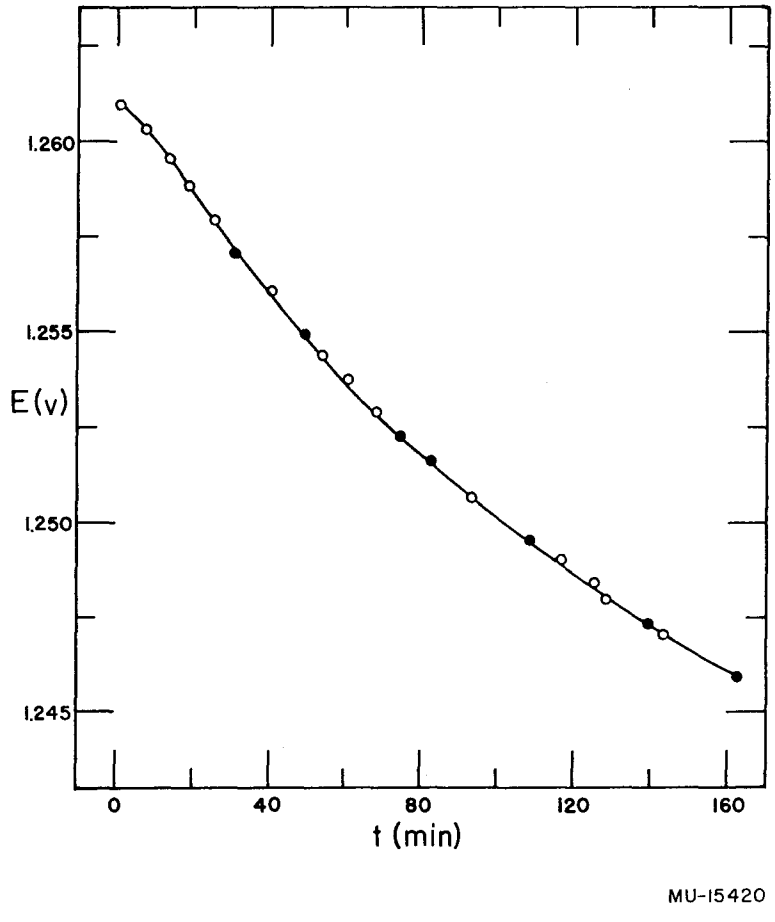

Fig. 18. The emf-time curve of Experiment V-C-1. Measurements made immediately after stirring are denoted by ●.

Performing the operation Eq. (6) - Eq. (4) + 2 x Eq. (2) - Eq. (7), one finds

$$HOI \underset{\longleftarrow}{\xrightarrow{K_{HOI}}} H^+ + IO^- \quad [K_{HOI} = K_{H_2O}^2 K_6 / K_2 K_7 = 2.3 \times 10^{-11}]. \quad (34)$$

Therefore the ionization constant of HOI (Eq. (34)) is 2.3×10^{-11}.

The accuracy of the ionization constant of HOI calculated above also depends on the precision of the hydrolysis constant of iodine. The value used here was from Allen and Keefer.[2] Values reported by some other investigators deviate considerably.[25,26]

(4) Discussion of the EMF Measurements

In comparison of the result for K_2 (Eq. (4)) from emf measurement with that from the spectrophotometric study, one notices that they are nearly, although not exactly, the same. As mentioned earlier, the K_2 value from emf measurement was obtained by the use of a gold electrode in the I^- - IO^- compartment. The platinum electrode used in the experiments of Table XIII gave lower values of K_2. For example the value of E_0(cell) of Experiment V-A-2 from the platinum electrode was 5.00 mv smaller than that from the gold electrode. This might be due to a reaction catalyzed by platinum as for example the disproportionation of the IO^-. The solution in the vicinity of the electrodes could then have a different composition than the bulk solution, and concentration polarization would result. The emf reading would then be influenced by stirring. There is also the possibility that the platinum electrode has a different response from the gold electrode to intermediate species formed from the disproportionation of IO^-, thus leading to a different emf. A new, pure, shiny platinum electrode did not improve the deviation from the gold electrode. Therefore it seemed unlikely that the trouble was due to impurities in the electrode.

Attempts were made to find conditions such that I_2OH^- would be the predominant species in order to get more evidence for its presence. Spectrophotometrically one was not able to study the absorption of I_2OH^- without getting interference from I_3^-, which absorbs very strongly in the wavelength region of this investigation. Similarly, difficulty was experienced in the emf measurement of a reaction mixture with relatively high I_2OH^-. The following initial concentrations were used:

$$(OH^-)_{in} = 0.1000 \text{ M};$$

$$(ClO^-)_{in} = 2.000 \times 10^{-4} \text{ M};$$

$$(I^-)_{in} = 0.7560 \text{ M};$$

$$(Cl^-)_{in} = 0.2496 \text{ M}.$$

From the known values of K_1 and K_2, it was calculated that the concentration of I_2OH^- would be equal to that of IO^-, and because of a low initial concentration of IO^-, its disproportionation should be quite slow even with the comparatively high ratio of $(I^-)/(OH^-)$. It was found that the emf readings of both the platinum and gold electrodes were appreciably affected by stirring. Contrary to the experiments of Table XIII, the value of K_2 using the platinum electrode was found to be closer to the value of K_2 reported in Table XIII than that from the gold electrode, although even the former was only about one-third of the value of K_2 reported in Table XIII. The cause of the deviation was probably not due to impurities in the solution or accidental contamination of the electrodes because, following disproportionation of the IO^-, the addition of fresh ClO^- to the decomposed solution to start a new run gave the same results within experimental error. The most likely explanation is that the two electrodes respond differently to the intermediate species from the

disproportionation of IO^-, or that the electrodes are catalyzing the disproportionation to some extent. It is to be hoped that further emf studies will be carried on in the near future.

ACKNOWLEDGMENTS

The author wishes to express her deep appreciation to Professor Robert E. Connick, who suggested this study and who has given thoughtful guidance, advice, and inspiration throughout the course of this investigation; to her fellow graduate students, particularly Dr. Claude P. Coppel, for their help and encouragement; and to Mrs. Jane Waite for her contribution to the progress of this project.

Thanks are also due to the Frank M. Hsu Scientific Fellowship from the China Institute in America and James M. Goewey Fellowship from the University of California, which made graduate study at the University of California possible.

Gratitude is felt for the financial support through the University of California Radiation Laboratory from the U. S. Atomic Energy Commission.

BIBLIOGRAPHY

1. R. P. Bell and E. Gelles, J. Chem. Soc. (London) 1951, 2734.

2. T. L. Allen and R. M. Keefer, J. Am. Chem. Soc. 77, 2957 (1955).

3. Hubert T. S. Britton, Hydrogen Ions, Ed. IV, Vol I, (D. Van Nostrand, Princeton, 1956).

4. E. L. C. Forster, J. Phys. Chem. 7, 640 (1903).

5. Anton Skrabal, Monatsh. Chem. 32, 167 (1911).

6. C. H. Li and C. F. White, J. Am. Chem. Soc. 65, 335 (1943).

7. Harold L. Friedman, J. Chem. Phys. 21, 319 (1953).

8. A. D. Awtrey and R. E. Connick, J. Am. Chem. Soc. 73, 1842 (1951).

9. K. G. Stern and D. DuBois, J. Biol. Chem. 116, 575 (1936).

10. John F. Below, Rapid Reactions: Kinetics of the Formation of the Ferric Thiocyanate Complex (Thesis), UCRL-3011, June 1955.

11. Farkas, Lewin and Bloch, J. Am. Chem. Soc. 71, 1988 (1949).

12. M. Anbar and H. Taube, J. Am. Chem. Soc. 80, 1073 (1958).

13. John O. Edwards, Chem. Revs 50, 455 (1952).

14. Robert E. Connick, J. Am. Chem. Soc. 69, 1509 (1947).

15. W. C. Bray and E. L. Connolly, J. Am. Chem. Soc. 33, 1485 (1911).

16. G. Horiguchi and H. Hagisawa, Bull. Inst. Phys. Chem. Research (Tokyo) 22, 661 (1943).

17. C. Herbo and J. Sigalla, Anal. Chim. Acta 17, No. 2, 199 (1957).

18. Wendell M. Latimer, The Oxidation States of the Elements and Their Potentials in Aqueous Solutions, Ed. II, (Prentice-Hall, New York, 1952).

19. M. Davies and E. Gwynne, J. Am. Chem. Soc. 74, 2748 (1952).

20. Linus Pauling, The Nature of the Chemical Bond, Ed. II, (Cornell Univ. Press, Ithaca, N. Y., 1940).

21. George E. Kimball, J. Chem. Phys. 8, 188 (1940).

22. George C. Pimentel, J. Chem. Phys. 19, 446 (1951).

BIBLIOGRAPHY

(contd.)

23. Joseph W. Kennedy, The Hydrolysis of Iodine and a Reaction with "Propanol", BNL-30, 1949.

24. Duncan A. MacInnes, The Principle of Electrochemistry, (Reinhold, New York, 1939).

25. Adolf Fürth, Z. Electrochem. 28, 57 (1922).

26. Anton Skrabal, Ber. 75B, 1570 (1942).

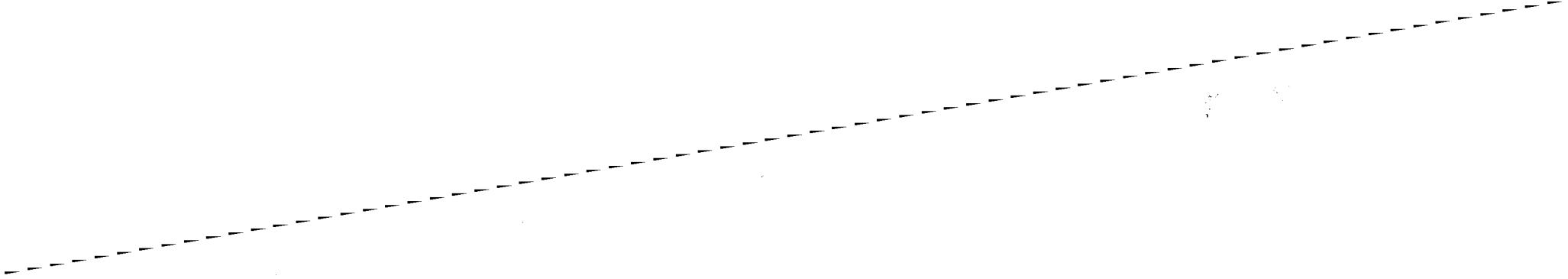

BIBLIOGRAPHY

(contd.)

23. Joseph W. Kennedy, The Hydrolysis of Iodine and a Reaction with "Propanol", BNL-30, 1949.

24. Duncan A. MacInnes, The Principle of Electrochemistry, (Reinhold, New York, 1939).

25. Adolf Fürth, Z. Electrochem. 28, 57 (1922).

26. Anton Skrabal, Ber. 75B, 1570 (1942).